M 2022

U.PORTO
FEUP FACULDADE DE ENGENHARIA
UNIVERSIDADE DO PORTO

PREPARATION AND FUNCTIONALIZATION OF CARBON MATERIALS FROM SUGARCANE MOLASSES FOR APPLICATION IN CATALYSIS

BERNARDO BASTOS SILVA

MASTER THESIS IN CHEMICAL ENGINEERING
PRESENTED TO THE FACULTY OF ENGINEERING
OF THE UNIVERSITY OF PORTO

Master in Chemical Engineering

Preparation and functionalization of carbon materials from sugarcane molasses for application in catalysis

Master dissertation

of

Bernardo Bastos Silva

Developed within the course of the Dissertation

held in

RAR / LSRE-LCM

Supervisor at FEUP: **Drª. Katarzyna Morawa Eblagon**

Joint supervisor at FEUP: Prof. Dr. M. Fernando R. Pereira

Coordinator at RAR: **Eng. José Manuel Chorão**

U.PORTO
FEUP FACULDADE DE ENGENHARIA
UNIVERSIDADE DO PORTO

DEPARTAMENTO DE
ENGENHARIA QUÍMICA

July 2022

Acknowledgment

This work was financially supported by LA/P/0045/2020 (ALiCE), UIDB/50020/2020 and UIDP/50020/2020 (LSRE-LCM), funded by national funds through FCT/MCTES (PIDDAC).

First, I would like to thank my supervisors, Drª. Katarzyna Eblagon, Eng. José Chorão and Prof. Dr. Fernando Pereira for guiding me through the course of this project, always lending a helping hand when needed, and enticing me to have curiosity when in pursuit of answers.

I would also like to thank RAR for the opportunity and LSRE-LCM for the very warm welcome I received and for making the workplace feel like home for the past months.

To Nuno, thank you for being the best lab partner, and you owe me 20 euros! Pay up. Thank you for never making me feel bad for showing up late, cause you showed up later.

To my mother, my father, and my brother, thank you for the values that you passed on to me and for the never-ending love we all share within our household. Without you, none of this would be possible. Thank you for allowing me to be who I am, and for loving me regardless of my decisions in life.

To my grandparents, thank you for raising me, for all the lunches and snacks, for all the love, for always being by my side whenever I needed and for being my biggest role models in life. To you, I leave you with this expression, “Grandparents have ears that truly listen, arms that always hold, love that’s never-ending, and a heart that’s made of gold”.

To my girlfriend, Cláudia, thank you for the past year, and thank you in advance for the years to come, for always allowing me to be me, for introducing me to Paula, Nala, and Romeu, and, for always staying true to your values and holding me accountable when I stray off mine. I am grateful for our past travels and looking forward to all our future endeavors.

To my group of friends, Ricardo, Miguel, Luis, Hugo, Mark, Diogo, Maria, Anita, Mariana, and Mara, thank you so much for accompanying me throughout this entire journey, for all the laughs, all the love, all the parties, all the trips, and all the emotional support. Thank you for being a part of my journey and for allowing me to be a part of yours.

Drª. Katarzyna Morawa Eblagon, supervisor of this dissertation is an integrated member of LSRE-LCM - Laboratory of Separation and Reaction Engineering – Laboratory of Catalysis and Materials, financially supported by LA/P/0045/2020 (ALiCE), UIDB/50020/2020 and UIDP/50020/2020 (LSRE-LCM), funded by national funds through FCT/MCTES (PIDDAC).

Abstract

This project focuses on the valorization of sugarcane molasses, a by-product of the sugar refining industry, by converting it into carbon materials using the hydrothermal carbonization process (HTC). Molasses is widely produced on a global scale, amounting to a yearly production of 50 million tons worldwide, and it is a promising precursor for the HTC process. The prepared carbon materials were functionalized with Brønsted acid sites in order to apply them as solid acid catalysts in the model reaction of fructose dehydration to 5-hydroxymethylfurfural (HMF). It is underlined that, to date, no articles have been published detailing this kind of valorization of molasses.

In this project, an optimization of the HTC process was carried out, by testing different water to molasses weight ratios (1:1, 1:2, 2:1) and different carbonization temperatures (170 ºC, 180 ºC, 190 ºC). For further functionalizations, the material with a 1:1 water to molasses weight ratio carbonized at 180 ºC was selected as a starting point. The material was functionalized with Brønsted acid sites by applying several procedures such as: high-temperature carbonization, in N_2 and CO_2, gas phase oxidation with 5 % (v/v) O_2/N_2, impregnation with H_2SO_4 and H_3PO_4, and liquid-phase oxidation with HNO_3.

The developed materials were characterized by several techniques such as: Elemental analysis, XPS, SEM/EDS, TGA, N_2 adsorption/desorption at -196 ºC, and were tested in the fructose dehydration to HMF, carried out at 180 ºC, continuously stirred at 600 rpm, with 3 bar of CO_2 of initial pressure for 2 hours.

Results from the catalytic performance showed that materials with phosphorus, sulfur and oxygen surface functionalities, as shown by elemental analysis and XPS, performed better than the material with high surface area, which did not show any withstanding effect. Finally, the material treated with H_3PO_4 recorded a yield of 53 % and a selectivity of 56 %, and it was the best catalyst in this work.

Keywords: Carbon catalyst, sugarcane molasses, hydrothermal carbonization, dehydration, Brønsted acid sites

Resumo

O foco deste projeto consiste na valorização de melaço proveniente da cana-de-açúcar, um subproduto da indústria de refinação de açúcar, através da sua conversão em materiais de carbono, utilizando o processo de carbonização hidrotérmica (HTC). O melaço é largamente produzido à escala global, ascendendo a uma produção anual de 50 milhões de toneladas mundialmente, sendo ainda um precursor bastante promissor para o processo de HTC. Os materiais de carbono preparados durante este projeto foram funcionalizados com sítios ácidos de Brønsted, de forma a serem posteriormente aplicados como catalisadores sólidos ácidos na reação de desidratação da frutose para produção de 5-hidroximetilfurfural (HMF). É de sublinhar que, até à data de escrita deste projeto, nenhum artigo foi ainda publicado detalhando este tipo de valorização do melaço.

Neste projeto, foi testada a otimização do processo de HTC, através do teste de diferentes rácios água/melaço (1:1, 1:2 e 2:1) e de diferentes temperaturas de carbonização (170 ºC, 180 ºC e 190 ºC). Para as funcionalizações posteriores, o material com rácio água:melaço 1:1 carbonizado a 180 ºC foi escolhido como ponto de partida. Este catalisador foi, então, funcionalizado com sítios ácidos de Brønsted através da aplicação de diferentes procedimentos, como é o caso da carbonização a altas temperaturas em atmosfera de N_2 ou CO_2, oxidação em fase gasosa com 5 % (v/v) O_2/N_2, impregnação com H_2SO_4 e H_3PO_4, e oxidação na fase líquida utilizando HNO_3.

Os materiais aqui desenvolvidos foram caracterizados por diversas técnicas, entre as quais análise elementar, XPS, SEM/EDS, TGA e adsorção/dessorção de N_2 a -196 ºC, sendo posteriormente testada a sua performance catalítica na desidratação da frutose a HMF durante 2 h a 180 ºC, com agitação contínua a 600 rpm e pressão inicial de CO_2 de 3 bar.

Os resultados da performance catalítica demonstraram que os materiais cuja superfície havia sido funcionalizada com fósforo, enxofre e oxigénio demonstraram resultados mais interessantes do que os restantes, cuja área superficial superior não relevou ter qualquer efeito. O catalisador que obteve os melhores resultados consistiu no material tratado com H_3PO_4, demonstrando um rendimento de 53 % e uma seletividade de 56 %.

Palavras-chave: Catalisadores de carbono, melaço de cana-de-açúcar, carbonização hidrotérmica, sítios ácidos de Brønsted

Declaration

I hereby declare, under word of honor, that this work is original and that all non-original contributions are indicated, and due reference is given to the author and source

Bernardo Silva

4th July, 2022

Index

List of Figures

List of Tables

Notation and Glossary

A	Area occupied by an adsorbed molecule	m^2
BE	Binding energy	eV
C	BET constant	
f	Severity factor	
m	Mass of solid	g
n	Number of moles of fructose	mol
N	Avogadro's constant	
P	Equilibrium pressure	bar
P_0	Saturated vapor pressure	bar
r^2	Correlation factor	
S_{BET}	BET specific surface area	$m^2 \cdot g^{-1}$
t	Reaction time	s
T	Temperature	K
V	Chemisorbed volume	m^3
V_m	Volume of a monolayer	m^3
V_M	Molar volume	$m^3 \cdot mol^{-1}$
X	Cumulative conversion	%

Indexes

0	Time of 0 min	min
max	Maximum mass loss	
x	time	min

List of Acronyms

ATR	Attenuated total reflection
BET	Brunauer–Emmett–Teller
CEMUP	Centro de materiais da Universidade do Porto
CSTR	Continuous stirred-tank reactor
DOE	Department of Energy
DTG	First derivative of TGA
EDS	Energy dispersive X-ray spectroscopy
FTIR	Fourier transform infrared spectroscopy
HMF	5-Hydroxymethylfurfural
HPLC	High performance liquid chromatography
HTC	Hydrothermal carbonization
ICP	Inductively coupled plasma
LSRE-LCM	Laboratory of Separation and Reaction Engineering – Laboratory of Catalysis and Materials
OES	Optical emission spectroscopy
RAR	Refinaria de Açúcar Reunidas
RI	Refraction index
SCM	Sugar cane molasses
SEM	Scanning electron microscopy
TGA	Thermogravimetric analysis
TPD	Temperature programmed desorption
UV	Ultraviolet
WL	Weight loss
XPS	X-ray photoelectron spectroscopy

1 Introduction

1.1 Framing and presentation of the work

The world has been experiencing a large increase in population during the last several decades[1]. As cities and economies grow, so does the amount of solid waste produced by households and businesses[1]. Municipal solid waste is growing, and it contains a high proportion of organic waste, which contributes to greenhouse gas emissions and other pollutants in the air. The world's population is expected to grow at a pace of 1.05 % each year, so that, by 2057, it would reach over ten thousand million people. As a consequence, the quantity of waste created will continue to rise[2]. Municipal and industrial solid waste processing has been regarded as critical to reduce the aforementioned consequences.

This project focuses on the valorization of a sugar industry waste, namely sugar cane molasses (SCM). It is worth noting that molasses made from beetroot sugar, which is mostly produced in the northeast of Europe, also exists[3], but will not be considered in this project. Molasses is generated all over the world as a by-product of sugar extraction and refining, from which no more sugar can be extracted by crystallization[4]. It is mostly used for animal feeding because of its composition, which makes it a good source of energy for ruminants[5]. SCM is also utilized on a large scale for synthesis of bioethanol in Brazil[6], for example. This strategy has been tested in various countries and has shown promising results[7,8].

SCM is made out of water (23.2 %), sucrose (48.8 %), glucose (5.29 %), fructose (8.07 %), ash (13.7 %), and other substances (< 1 %)[9]. However, because molasses is an agricultural product, its constitution varies[10], depending on where the sugar cane is grown, making it difficult to determine its exact composition.

In 2019, the sugar cane molasses market was valued at 709 million euros[11], making it the world's 2253rd most traded product. The biggest exporters of molasses at the time were India, Thailand, Indonesia, and Guatemala, which account for 46 % of the total global exports. On the other hand, the biggest importers were the United States of America, the Philippines, the United Kingdom, and South Korea, accounting for 50 % of molasses' global imports[12]. Worldwide yearly production of this substance is reported to be about 50 million tons[13].

Narrowing the scope to Portugal, in 2017, 740 tons[14] of molasses were produced. Furthermore, in 2019, Portugal exported roughly 765 tons of molasses[15], with the main importers being Spain, France, the United Kingdom, and the Netherlands. This exportation amounted to 228 000 euros[15].

This project was carried out in a collaboration between Laboratory of Separation and Reaction Engineering – Laboratory of Catalysis and Materials (LSRE-LCM) and one of the main sugar manufacturers in Portugal, *Refinarias de Açúcar Reunidas* (RAR), integrated in the RAR group. This group has an estimated revenue of 732 million euros (2020), with 69 million euros from sugar refining. RAR sugar amounts to 34 % of all the sugar in Portugal and 9 % in Spain. Annually, RAR has a production capacity of about 170 000 tons of refined sugar, which is not used to its totality, generating 4600 tons of molasses per year. RAR sells their molasses at 150 euros per ton, meaning that annually, molasses brings them about 690 000 €. RAR sells SCM to manufacturers of cattle food.

The factory's sugar refining process can be summarized in Figure 1.1, where the main steps are shown. Each step is very complex and entails plenty of very expensive machinery.

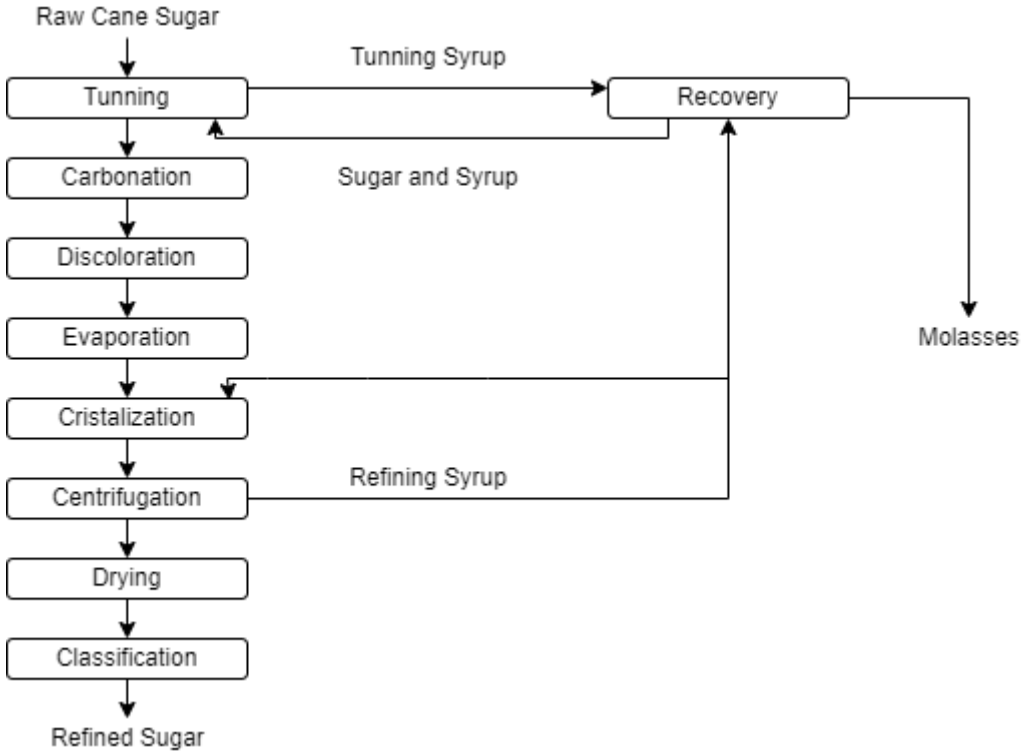

Figure 1.1: Flow diagram of sugar refining process followed by RAR.

The raw cane sugar is blended with tunning syrup in the tunning stage, and tunned sugar is produced after passing through a crusher and tunning centrifuges. This sugar is then combined with sweet water to create the tuning liquor, which is subsequently carbonated. The liquor is combined with milk of lime and carbonated in this phase. At the conclusion of this phase, carbonated liquor is created, which is then discolored by passing it through columns containing discoloration resins, which remove the color from the liquor. In the next stage, the liquor is concentrated by the evaporation of water. Cooking the liquor to a point of oversaturation crystallizes the sugar dissolved in it. This heated material is centrifuged to obtain wet sugar. The wet sugar is dried before being graded using a three-sieve method that separates the sugar

by size. Finally, SCM is obtained during the recovery process, from which no more sugar can be extracted.

As previously stated, the molasses market is quite vast, implying that a commodity that was formerly considered a waste has garnered attention and worth. It should be mentioned that if molasses were valorized in a better, more profitable, and sustainable way, this market might increase tremendously.

Sugary materials have been demonstrated to be viable raw materials for producing carbon materials using hydrothermal carbonization (HTC) in various investigations[16–19]. Carbon materials may also be activated via templating other activation processes, resulting in an increased surface area[19]. Functionalization of these materials, such as doping with nitrogen[20,21], sulfur, boron[22], phosphorus[7], or oxygen[20] can improve their catalytic characteristics. The synthesis of doped carbon catalysts from molasses using HTC and their application as solid catalysts in the fructose dehydration to 5-hydroxymethylfurfural (HMF) is detailed in this project.

1.2 Presentation of the company

RAR was founded in 1962, as a sugar refining company with a production capacity of 50 000 tons per year. Five years later, with the acquisition of licenses, rights, land and machinery, the production capacity increased to 75 000 tons per year. With expansion in sight, Acembex – Açúcar, embalagem e exportação, was created in 1970. In 1981, RAR Holdings was created, which is the company that, to this day, controls all RAR group's shareholdings. In 1987, RAR Imobiliária was founded, and it is currently a high-end real estate agency. Finally, in 2000 and 2007, the group acquired Colep and Vitacress Salads, respectively. All the aforementioned companies currently constitute RAR group.

In 2020 the group had a turnover of 732 million euros, with Colep being the highest grossing company, garnering 357 million euros split between Colep consumer products and Colep packaging. RAR sugar in particular had a turnover of 69 million euros in 2020. RAR group currently employs 4 200 people in their facilities.

Currently, the sugar refinery has an annual capacity of 160 thousand tons, which is normally not fully engaged, and it is responsible for 34 % of the sugar sold in Portugal, as well as 9 % of the sugar sold in Spain.

1.3 Contribution of the author to the work

The work carried out in partnership with RAR – Refinarias de Açúcar Reunidas which provided the samples of molasses to be used as carbon precursors in the present project.

First and foremost, this work provided insight on the potential of molasses as a precursor to produce carbon materials. As such, valorizing molasses to produce carbon materials for various applications can give additional revenue to RAR. The optimized hydrochars obtained from molasses could be possibly applied by RAR as adsorbents for the discoloration stage of their process, which is currently done using expensive polymers or activated carbon with high specific surface areas.

Furthermore, this work has shown that, for the dehydration of fructose to HMF reaction, surface chemistry has a much bigger impact on catalytic performance than the BET (Brunauer–Emmett–Teller) specific surface area of the materials.

Moreover, except for the SEM/EDS and XPS analyses which were done in the *Centro the Materiais da Universidade do Porto* (CEMUP), and the fitting of the XPS peaks, which was also done externally, the entirety of the work was done by the author.

1.4 Organization of the dissertation

The dissertation is divided into several chapters and subchapters. It begins with Chapter 1, which includes the introduction of the work. The background of this project describes the environmental problems faced by today's world, with the main focus being waste treatment and valorization, namely the sugar industry's most manufactured by-product, SCM. Furthermore, the worldwide and national SCM markets are referred, introducing the idea that SCM has a high market potential if it is valued in a sustainable and profitable way. Moreover, the sugar refining process used by RAR is detailed. The purpose of this work is also introduced in this Chapter, and it entails the production of carbon catalysts via hydrothermal carbonization (HTC) of molasses. These catalysts will be applied in the fructose dehydration to 5-HMF. The following Subchapter depicts a brief presentation of the company RAR – *Refinarias de Açúcar Reunidas*, and its many endeavors. Finally, it covers the author's contributions to the work presented in this thesis.

Chapter 2 covers the context and the state of the art, where the HTC process is detailed regarding its mechanism, as well as the influence of the reaction parameters and the type of feedstock used. Furthermore, Chapter 2 details the several steps that can follow catalysts production via biomass HTC, namely carbonization and activations of hydrochars using various methods. Moreover, Chapter 2 introduces the reaction of interest, which is fructose dehydration to HMF, and explains the necessity to functionalize the materials with Brønsted acid active sites.

Chapter 3 describes the experimental part of the work, which includes preparation, characterization, and catalytic testing of the prepared materials. This Chapter provides insight into the utilized equipment, experimental conditions, methods and approaches used.

Chapter 4 entails the main results of the experimental work. The main characteristics of the materials, including their chemical composition, stability against oxidation, BET surface area and, finally, their catalytic performances, are showed and compared. The conclusions are drawn linking the materials' characteristics and their catalytic performance in the fructose dehydration to HMF, which was used as model reaction.

In Chapter 5, the main conclusions of this research project are drawn and presented, as well as the future work proposed.

Finally, Chapter 6 denotes a closing overview regarding the work done by the author.

2 Context and State of the art

2.1 Hydrothermal Carbonization

It is critical nowadays to convert biomass into green carbon using methods other than pyrolysis. The study of mechanisms that allow for fine-tuning of the carbon molecular structure and morphology is crucial since it provides materials with their desired qualities. HTC has sparked interest in recent years due to its capacity to transform biomass into highly functionalized carbon materials.

The HTC process, however, is not new and has already been used for a long time, since it tends to mimic the natural formation of coal. Moreover, it is known as an economic approach due to the utilization of cheap biomass precursors, such as algae, xylan, grass, plants, sludge, compost, animal waste, agricultural residue, straw, wood, food and food waste, cellulose, municipal solid waste, lignin, yard waste, starch, xylose, glucose, paper and animal feed, to name a few[19]. Since molasses contains a mixture of carbohydrates[23], it is a good candidate for biomass precursor. Nevertheless, there are no previous works dealing with the production of carbon hydrochars or carbon materials via HTC using molasses as carbon precursor, and their application in the fructose dehydration to HMF. Thus, this dissertation documents the first attempts towards valorizing molasses to carbon materials and their application in heterogeneous catalysis.

HTC is a thermochemical process, carried out at mild processing temperatures ranging from 180 °C to 250 °C, under self-generated pressure, and using water as a solvent. Since the process is held in water, the carbon precursor derived from biomass does not require any preliminary drying step, allowing for a large saving of energy and time. It should be underlined that the energy required for this process is much lower when compared to that of pyrolysis and gasification, which yield similar products[24], as it is clear from the data present in Table 2.1. This table compares the characteristics of several thermochemical processes commonly used to produce carbon materials or hydrochars from biomass precursors. The hydrothermal carbonization clearly displays some economic advantages, as lower energy consumption due to lower temperature range, medium reaction time and no oxygen consumption. Other advantages of HTC are: low toxicological impact of materials and processes, the use of renewable resources, facile instrumentation and techniques, and excellent energy and atom economy[25].

Table 2.1: A comparison between several thermochemical processes used for carbon production[24]

Process	Conditions			Energy Products	Yields / %		
	Temperature / ºC	Reaction time	Oxygen input		Char	Liquid	Gas
Combustion	850-950	0.5-2 s	excess	Heat	15-20	-	80-90
Gasification	800-1000	10-20 s	limited	Syngas/heat	10	5	85
Fast pyrolysis	500	1 s	-	Bio-oil and biochar	12	75	13
Slow pyrolysis	400	h-weeks	-	Biochar and bio-oil	35	30	35
HTC	150-250	1-12 h	-	Hydrochar	50-80	5-20	2-5

Furthermore, HTC is the process that allows to obtain higher char yield (50 – 80 %), with the lowest gas emissions, and thereby it appears to be the most promising process to produce carbon materials.

Several studies have been conducted throughout the years to understand the mechanism of HTC using biomass-derived precursors. Even though the biomass primarily consists of carbohydrates, the composition of saccharides may differ among various raw materials. Generally, the reaction mechanism involves the following reactions: hydrolysis[24], dehydration[24], decarboxylation[24], condensation[24], polymerization[24], and aromatization[24], as it is detailed in Figure 2.1.

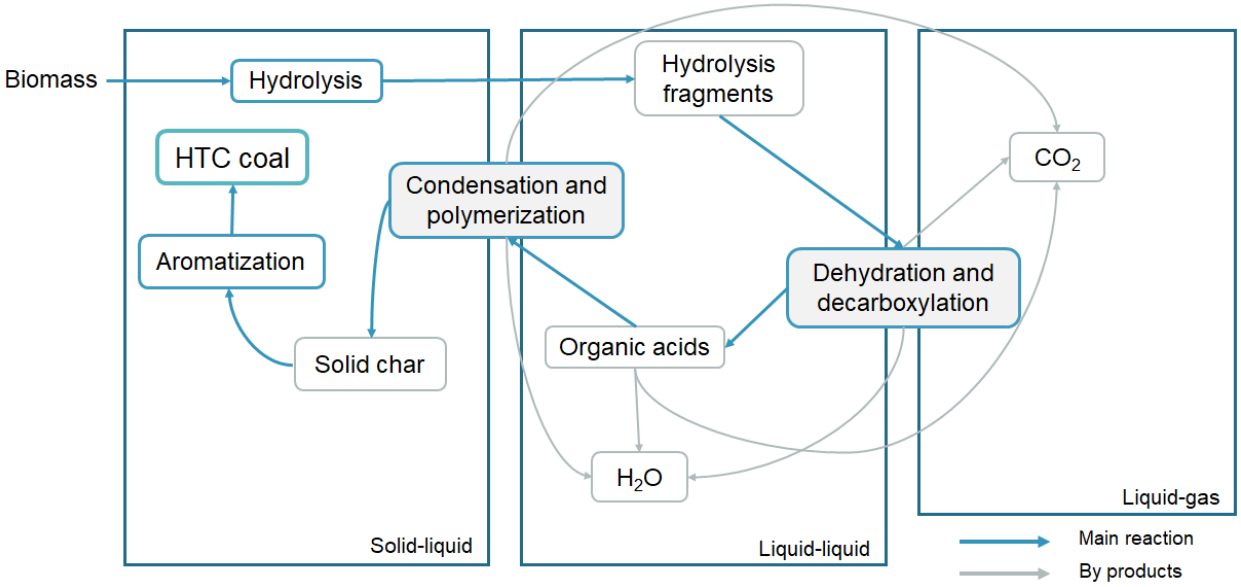

Figure 2.1: Hydrothermal carbonization mechanism scheme, adapted from the work of Pauline et al [24]

Generally, these steps begin with the hydrolysis of cellulose and hemicellulose chains into their respective monomers, mainly glucose and other secondary sugars. Nonetheless, this occurs when the feedstock is lignocellulosic biomass, which is predominantly constituted by cellulose, hemicellulose, and lignin. In this project, the raw material is molasses, which does not have cellulose in its constitution as it is stated in Subchapter 1.1., and thus, the hydrolysis occurs

upon sucrose, breaking the glycosidic bond into hexoses (*i.e.*, glucose and fructose)[26]. The hexoses, regardless of their source, are then dehydrated into 5-HMF and furfural, respectively[27]. Decarboxylation also occurs to remove carbon dioxide (CO_2) from the mixture. From this point in the process, decomposition of the compounds to lower molecular weight hydrocarbons may arise. Alternatively, condensation and aromatization reactions can take place, to form hydrothermal carbon. It is noteworthy that these reaction steps are not consecutive but parallel reactions[27].

The HTC can be described as an autocatalytic process since, during the decomposition of sugars to HMF and furfural, levulinic and formic acids are formed, which act as homogenous catalysts and promote sugar dehydration[26].

2.2 Influencing Parameters

The HTC process can be influenced by various factors, such as temperature, reaction time, ratio between feedstock and water, as well as the type of feedstock used as raw material. These parameters may alter the final material morphology, carbon yield, and its chemical properties.

2.1.1 Type of Feedstock

Since HMF and furfural are products of the dehydration of hexose and pentose sugars, respectively, they are the building blocks in the formation of hydrothermal carbon materials (hydrochar). Taking this into consideration, it is plausible to predict that hydrochars will have similar morphology regardless of the feedstock, as long as they have pentoses and hexoses[19]. Titirici *et al.*[28] noted that carbon spheres obtained from the hydrothermal treatment of xylose and furfural have no notable difference in their shape. Furthermore, when comparing the ones obtained from hexose and HMF, the shapes were remarkably similar.

Moreover, feedstock properties have been shown to influence carbon yields as well as the chemical composition of hydrochars. Several studies have shown that, in comparison to process conditions (reaction time and temperature), feedstock properties are more influential on carbon loading and chemical composition[29]. However, it is noteworthy that, on average, carbon yields range between 30 to 50 %[29].

2.1.2 Reaction time, temperature, and concentration

Reaction time and temperature have also been shown to influence the HTC process[30,31], affecting material morphology, size, and carbon yield. Mao *et al.*[31] conducted a study where they reported the influence of reaction time, temperature, and concentration on the morphology of carbon spheres. The tests were executed at five different temperatures ranging between 220-290 ºC. For the lowest temperature, it was noticed that the hydrochar had a similar morphology to the raw material. By increasing the temperature up to 270 ºC, the spheres

became larger, and with better dispersion, although for higher temperatures, 290 ºC, the particles tended to aggregate, and cross-linking occurred. Furthermore, keeping the temperature and concentration steady, the effect of the reaction time was tested. Results showed that, for reaction times up to 3 hours, only slight differences were noted since hydrolysis might have just been starting. With increasing reaction times, the carbon spheres became larger and more defined.

Finally, the feedstock concentration was analyzed, and the results showed that, for concentrations between 0.04 g mL^{-1} and 0.06 g mL^{-1}, more uniform spherical particles started to form with the increase in concentration. On the other hand, by further augmenting the concentration of feedstock, the particles began to bind, ultimately creating a cluster of agglomerated spheres.

In a similar study, Romero-Anaya *et al.*[30] reported that sugar derived carbon spheres achieved bigger and more uniform sizes with extended reaction time from 12 to 24 hour range. The authors reported that, at 12 hours, spherical carbons were not yet well defined, while, at longer reaction times (> 24 hours), no further changes in size and morphology of the carbon spheres took place.

In addition, Sevilla *et al.*[32] and Mao *et al.*[31] reported independently the increase in the hydrochar yield and in the diameter of carbon microspheres by increasing precursor concentration, reaction time, or temperature. The aforementioned studies also indicated that reaction time, temperature, and feedstock concentration all have a substantial effect on hydrochar morphology.

Considering carbon yield, Funke *et al.*[18] developed an equation in which the effects of both temperature, T, and reaction time, t, are taken into account in one parameter alone, named the severity factor, f, described in Eq. 2.1.

$$f = 50t^{0.2} \times exp\,(-3500/T) \qquad \textit{Eq. 2.1}$$

In a review paper regarding hydrothermal carbonization, Nicolae *et al.*[19] collected data from numerous papers where a wide range of feedstocks was utilized, for different severity factors. In Nicolae's review, the authors presented a comparison between the influence of the process conditions and the feedstock. The data was organized taking into consideration increasing severity factors; however, no trend was reported regarding carbon and hydrogen content. Thus, it can be concluded that the type of feedstock has a greater effect on hydrochar carbon loading than process conditions.

2.2 Activation methods/ Activated Carbon

The product of the HTC process, under regular conditions, is called hydrochar. Because of its low surface area, hydrochars can be activated to broaden their range of applications, such as: adsorbents for dyes[33], heavy metals[34] and volatile compound[35], electrode materials for electrochemical capacitors[36] and supercapacitors[37] and gas[38] storage. The activation process enhances the surface area of a given carbon material, creating void spaces (pores) in its structure. Due to its porosity, activated carbon is considered as a particularly unique material. The close proximity of the carbon atoms in the pores, provides the pores with strong Van Der Waals interactions and zero electron density[39], equipping the activated carbons with great adsorption capabilities. This is why activated carbons are broadly used as adsorbents[40,41].

There are several methods available to introduce pores into a carbon structure, which can be divided into two categories, templating, and activation methods.

2.2.1 Templating methods

HTC is characterized as a rather versatile process, thus, the materials obtained from it can be combined with templating methods. There are two types of methods, soft or endo templating, and hard or exo templating.

Soft templating

This method consists of using an amphiphilic molecule, like a surfactant or a block-copolymer, which has a high molecular weight and forms self-assembled micelles in the solvent with a carbon precursor, creating a mesophase[42]. This mesophase undergoes stabilization through thermal treatment, while concentration, temperature, and pH values can be controlled to optimize the process.

Small surfactant molecules such as octadecyltrimethylammonium ($CH_3(CH_2)_{17}N^+(CH_3)_3$), hexadecyltrimethylammonium ($CH_3(CH_2)_{15}N^+(CH_3)_3$), and tetradecyltrimethylammonium ($CH_3(CH_2)_{13}N^+(CH_3)_3$), as well as block copolymers the likes of Polystyrene-b-Poly(4-vinylpyridine) and Pluronic®[43].

It is noteworthy that, under hydrothermal conditions, the carbon precursor is transformed into carbon at the interface of the template. Moreover, when compared with hard templating, this method reduces reaction time, and it is much simpler[44].

Hard templating

This method is based on the structure replication approach, using sacrificial templates, such as mesoporous silica, zeolites, clay materials, and metal-organic frameworks for example[45]. The hard templating approach is based on a mixture of a carbon precursor with a hard template. Thus, the carbon precursor will infiltrate into the structure of the template and will be

carbonized at high temperatures within the pores, turning into a continuous carbon framework[45].

When compared with soft templating, hard templating allows for a better control over the carbon structure. The essential difference between the two methods is that, while soft templating relies on the cooperative assembly between the surfactant and the inorganic phase, in hard templating the objective is to replicate a certain solid structure. Hard templating is advantageous because the products are easy to control since the templates have fixed structures[46]. However, this method does not come without its drawbacks, since, in some cases, the pores it creates have been known to collapse[45].

2.2.2 Activation methods

Regarding activation methods, there are two distinct ones, physical activation and chemical activation, both reliable to introduce pores within the carbonaceous structure, despite only the latter can dope the carbon surface with heteroatoms.

Physical Activation

Physical activation is a two-stage process that features the carbonization stage in the presence of an inert gas (N_2 or Ar) followed by the activation stage with the aid of an oxidizing agent in the gas phase (O_2, CO_2, air or H_2O steam). The physical activation is normally done in the temperature range of 800–1200 °C[47]. Regarding oxygen or air treatments, it is critical to consider how exothermic the oxidation is, and thus, it is critical to control the temperature, or else, all the carbon material will end up being burned off. For that reason, carbonizations are usually done using steam or carbon dioxide to limit the burn-off of the material.

In the present work, however, the main objective was to synthetize carbon materials for application in catalysis. In the chosen application, the extremely high surface areas are not indispensable. Nevertheless, physical activation using CO_2 was applied to hydrochars in order to check the possibility of broading these materials' applications to other fields, where high surface area is necessary, like dye removal or selective gas adsorption.

Chemical activation

In chemical activation, the HTC carbon is mixed with an acid, a base, or even a salt before carbonization. The most common chemicals utilized to activate a hydrothermal carbon are KOH[48,49] and NaOH[50], which are strong alkaline activating agents, while K_2CO_3[51] and Na_2CO_3[52] constitute the second type or middle alkaline activating agents. Finally, there's a third type, or weak activating agents, namely K_2SiO_3[53], Na_2SiO_3[54], $K_2B_4O_7$[54], $Na_2Al_2O_4$[54], $C_4H_6K_2O_7$[55], $C_6H_5K_3O_7$[56] and K_3PO_4[57]. On the other hand, there are also acidic activating agents, which were utilized in this work, such as H_3PO_4[58,19], $H_4P_2O_7$[59], H_3PO_3[60], HPO_3[61], H_2SO_4[16], and HNO_3[62]. Nowadays, chemical

activation with KOH is the most commonly used method to produce highly porous carbon materials, that allows to achieve surface areas in the range of 2000 $m^2 \cdot g^{-1}$ [49].

HTC Carbon in catalysis

Hydrothermal carbon has shown to have several viable applications such as energy storage[63], supercapacitor electrode materials[64], wastewater treatment[65], dye removal[66], and, heterogeneous catalysis[19], the latter being the focus of this project. The wide application of these materials justifies the approach of the current project to valorize molasses to hydrochars.

Heterogeneous Catalysis

Heterogeneous catalysis, that is the intended application of the hydrochars produced in the current work, deals with the ability of solid surfaces to make and break bonds between molecules[67]. Heterogeneous catalysis involves the systems in which the reaction takes place in liquid or gas phase while the catalyst used is in the solid phase. During the catalysis, at least one of the reactants adsorbs on the surface of the solid catalyst, where it gets activated, which is followed by the surface reactions to form adsorbed products. Finally, in the last step, the products desorb from the catalyst surface[67].

Heterogeneous catalysis allows the catalyst to be reused since it does not dissolve during the reaction, and thus it provides facile extraction of the catalyst from the reactional mixture[68]. Thus, the heterogeneous catalysts can be recycled, as opposed to their homogeneous counterparts. Furthermore, when comparing heterogeneous catalysts with their homogeneous counterpart, the former is less energy-consuming and consequently less corrosive to the surrounding equipment[68].

On the other hand, the drawbacks of heterogeneous catalysts are related to their low diffusivity, heat transfer issues, and usually lower selectivity when compared to their homogenous counterparts. However, there are some solutions to tackle the aforementioned issues[69]. Diffusivity can be improved by increasing the porosity of the catalysts. Finally, by optimizing the catalyst manufacturing process and tuning its steric and electronic properties, significant tunning of the catalysts surface can be achieved.

To conclude, from the economical and environmental point of view, the clear recycling advantages render heterogeneous catalysts as the better option.

2.2.3 HMF production

The goal of this project is to produce carbon catalysts via HTC using SCM as carbon source. These materials will be later functionalized to obtain carbon catalysts with Brønsted acid active sites. Thus, the prepared catalysts, with different types and strengths of Brønsted acid sites, will be assessed in the dehydration of fructose to 5-hydroxymethylfurfural.

HMF has been recognized by the Department Of Energy (DOE) as one of the versatile platform chemicals[70] since 2010 and it is considered one of the top 12 building blocks for biorefinery. HMF contains a furan ring, and two functional groups, aldehyde and hydroxyl groups[71], which makes it a suitable building block that can be converted to many other value-added products, namely alkoxymethylfurfurals, 2,5-furandicarboxylic acid, 5-hydroxymethylfuroic acid, bishydroxymethylfuran, and 2,5-dimethylfuran. The aforementioned furan derivatives have many potential applications in biopolymers, biofuels or pharmaceuticals[71]. Additionally, HMF can also be converted to many non-furan fine chemicals such as: levulinic acid, adipic acid, 1,6-hexanediol, caprolactam, and caprolactone[71]. However, it has been difficult to achieve a process with high selectivity and a high isolated yield, rendering the price of HMF unacceptably high.

The fructose dehydration to HMF with rehydration to levunic and formic acids is detailed in Figure 2.2.

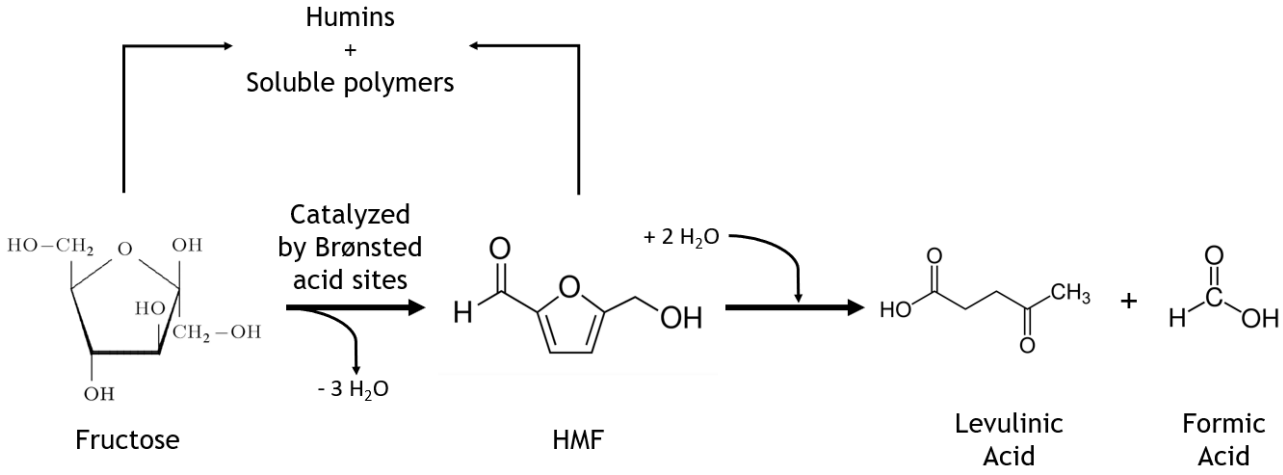

Figure 2.2: Fructose dehydration to HMF[72]

HMF synthesis occurs through the dehydration of hexoses with the aid of Brønsted acid sites. HMF is formed by the loss of three water molecules from fructose[73]. The most used carbohydrates to produce this platform chemical are glucose and fructose. It can be easily obtained from fructose, and fructose can be produced from glucose by various methods, including enzyme catalysis[73]. Some polysaccharides containing glucose or fructose monomers such as starch, cellulose, inulin or sucrose can also be used as a substrate for this reaction.

Despite fructose being the best substrate for this reaction, it is not easily available and therefore it is not cheap. A better option for a mass production of HMF is biomass-derived glucose, which is around 5 times cheaper than fructose and can be obtained from a wide range of biomass feedstocks, including food waste and industrial by-products such as SCM.

As it can be seen in Figure 2.2, there are some side reactions taking place such as cross polymerization, which forms brown soluble polymers as well as humins, which are insoluble

polymers. Furthermore, rehydration of HMF into a mixture of levulinic and formic acids can occur[72]. These unwanted reactions are the main challenge for the selective production of HMF from fructose[73].

2.2.4 Heteroatom doping

Considering that the reaction of interest is catalyzed by Brønsted acids, functionalization of the hydrochars with this type of active sites should increase their catalytic performance. Compounds such as sulfuric acid[74], phosphoric acid[75] and nitric acid[76] can be used to treat the carbons and to introduce acidic functional groups, in the form of phosphoric groups, sulfonic, or oxygen funcionalities[76], respectively.

Villa *et al.*[75] reported that phosphorylated carbon catalysts have adequate activity for fructose dehydration and give a high HMF selectivity, with a relatively low amount of levulinic acid, formic acid, and humins as by-products. When compared to sulfonated carbons, phosphorylated carbons showed a lower catalytic activity, but a higher HMF selectivity, meaning that sulfonated carbons are more catalytically active and form more secondary products, leading to a decrease in HMF selectivity. Furthermore, it was shown that, by increasing the phosphorus concentration in the carbon material, the activity increased, and consequently, so did the number of secondary products. As a result, the selectivity to HMF decreased.

Zhao *et al.* [74], in a study regarding sulfonated catalysts for HMF production, tested the performance of a sulfonated catalysts on which H^+ were substituted by ion exchange with Na^+. Analyzing the limited performance of the substituted catalyst, it was demonstrated that the role of a protonic acid (Brønsted acid) in fructose dehydration to HMF is critical.

3 Materials and Methods

The present chapter covers the experimental work, from catalysts production, characterization methods, to the catalytic testing they underwent.

3.1 Material preparation

For material preparation, firstly, water and molasses (provided by RAR) were mixed using different mass ratios [1:1; 1:2; 2:1 (water: molasses)]. The mixtures were placed in a 70 mL Teflon reactor cup, which was placed in a stainless-steel reactor. The HTC reaction took place in a France Etuves vacuum oven, for 8 hours and at different temperatures and under self-generated pressure. The effects of the water to molasses ratio were studied by keeping the temperature of the process at 180 ºC. The influence of the temperature on the HTC was also studied, keeping the mass ratio between molasses and water at 1:1. The materials were abbreviated as HTC_x/y_T, where x/y is the water/molasses weight ratio used and T is the carbonization temperature. For example, material HTC_1/2_180 is a hydrochar produced by mixing water and molasses in a 1:2 water to molasses weight ratio and carbonized at 180 ºC. Thus, the following hydrochars were prepared: HTC_1/1_180, HTC_1/2_180, HTC_2/1_180, HTC_1/1_170 and HTC_1/1_190.

All these materials were washed with distilled water under a vacuum filtration until transparent filtration was obtained. Afterwards, the solvent used for washing was changed to ethanol and the procedure was repeated. When the materials were synthesized in the presence of acids, or post-treated with acids, the washing was carried out until the neutral pH value of the filtrate was obtained.

Since there was no noticeable difference in the carbon yield between different hydrochars, in the second part of this work, the HTC_1/1_180 sample was chosen as a representative hydrochar for post-synthetic functionalization. The detailed procedures used to functionalize the hydrochar with Brønsted acid sites are detailed in the current Chapter.

The materials derived from HTC_1/1_180 will be abbreviated to HTC followed with the abbreviation of the agent used for functionalization.

The HTC was carbonized under a 100 $cm^3 \cdot min^{-1}$ N_2 flow rate at 600 ºC for 2 hours, at a heating rate of 10 ºC $\cdot min^{-1}$ in a glass tube reactor using a Termolab furnace. The obtained material was labeled as HTC_Carb.

HTC_Carb was subsequently treated in a 100 $cm^3 \cdot min^{-1}$ flow rate of 5% (v/v) O_2/N_2 at 350 ºC for 3 hours using a glass tube reactor placed in a Termolab furnace, in order to introduce surface oxygen groups. This method led to the production of HTC_Carb_O_2.

Regarding acid treatments, material HTC_Carb was functionalized with 3 M H_2SO_4, using a ratio of 1 gram of carbon to 20 mL of acid. The mixture was placed in a 70 mL Teflon reactor cup, which was inserted in a stainless-steel reactor, and treated in the France Etuves vacuum oven at 150 ºC for 24 hours. The new material was washed with distilled water until a neutral pH was reached; then, the material was dried overnight. The obtained material was labelled HTC_Carb_H_2SO_4.

Furthermore, HTC_Carb was functionalized with HNO_3, by liquid phase oxidation, to introduce oxygen containing surface groups. In this treatment, 2 g of sample were placed in a Soxhlet extractor which was connected to a round bottom flask and a condenser. In the round bottom flask, 200 mL of 7 M HNO_3 were placed. The HNO_3 was heated to boiling temperature, the acid vaporized and went up the set up, bypassing the material; then, it condensed in the condenser and descended into the material in the Soxhlet extractor. Once the HNO_3 started boiling, this process was held for 2 hours. Afterwards, the material was washed with distilled water until a neutral value of pH was achieved. The final material was labelled HTC_Carb_HNO_3.

Moreover, to incorporate phosphoric surface groups, HTC was immersed in 5 M H_3PO_4, using a weight ratio of 1:2 hydrochar to phosphoric acid for 24 hours. Afterwards, the material was filtered and washed with distilled water until neutral pH was obtained, resulting in HTC_H_3PO_4. This material was further carbonized in a glass tube reactor, using a Termolab furnace at 600 ºC under a 100 $cm^3 \cdot min^{-1}$ flow rate of N_2 for 2 hours. The new material was named HTC_H_3PO_4_Carb.

Finally, HTC_Carb_CO_2, was produced by heating the HTC material in a glass tube reactor to 750 ºC under a 100 $cm^3 \cdot min^{-1}$ flow rate of N_2, then kept stable for 4 hours in an 85 $cm^3 \cdot min^{-1}$ flow rate of CO_2. Finally, the material was cooled down to room temperature under a 100 $cm^3 \cdot min^{-1}$ flow rate of N_2. The materials created in this work can be found summarized in Table 3.1.

Table 3.1: Summary of the materials produced and their methods

Material	Treatment method
HTC	Hydrothermal carbonization at 180 ºC for 8 hours
HTC_Carb	Carbonization under 100 $cm^3 \cdot min^{-1}$ of N_2 at 600 ºC for 2 hours
HTC_Carb_O_2	Gas phase oxidation with 100 $cm^3 \cdot min^{-1}$ of 5% O_2/N_2 at 350 ºC for 3 hours
HTC_CO_2	Treatment in 85 $cm^3 \cdot min^{-1}$ of CO_2 at 750 ºC for 4 hours
HTC_H_3PO_4	Impregnation with 5 M H_3PO_4 under continuous stirring for 24 hours
HTC_H_3PO_4_Carb	Impregnation followed by 600 ºC carbonization in 100 $cm^3 \cdot min^{-1}$ of N_2
HTC_Carb_H_2SO_4	Impregnation with 3 M H_2SO_4 in a vacuum oven at 150 ºC for 24 hours
HTC_Carb_HNO_3	Treatment with 7 M HNO_3 in liquid-phase oxidation for 2 hours

3.2 Characterization methods

The materials were characterized regarding their elemental composition, surface chemistry, morphology, porosity, and thermal stability to oxidation.

3.2.1 Thermogravimetric Analysis, TGA

Thermogravimetric analysis (TGA) is done to analyze the amount of inorganic material (ash) as well as the material's thermal stability towards oxidation, when performed in an air atmosphere. In air, when the temperature of the equipment reaches around 300 ºC, carbon monoxide and dioxide start to form, which consequently leads to the burn-off of organic matter. If the temperature is set high enough (900 ºC), it will leave only the ash behind. In this work, the goal was to analyze the thermal stability of the materials against oxidation; thus, they were analyzed in air. In this analysis, first, the equipment needed to stabilize. After stabilizing, the furnace was heated to 750 ºC with a 10 ºC·min^{-1} heating ramp. All TGA essays were done utilizing the Netzsch-Gerätebau GmbH - STA 409 PC Luxx Simultaneous thermal analyzer.

3.2.2 N_2 physisorption at -196 ºC

The interpretation of adsorption/desorption isotherms provides a plethora of information regarding the texture of the catalyst. Recurring to this method, the main parameters that can be assessed are specific surface area, pore size distribution, pore volume, and presence of hierarchical structures.

To determine the specific surface area, the BET equation, presented in Eq. 3.1, is used, where V (m^3) is the chemisorbed volume, V_m (m^3) is the volume of a monolayer, P_0 and P are the saturated vapor pressure and equilibrium pressure in bar, respectively, and C is the BET constant.

$$V = \frac{V_m C \frac{P}{P_0}}{\left(1 - \frac{P}{P_0}\right)\left(1 - \frac{P}{P_0} + C\frac{P}{P_0}\right)} \qquad \textit{Eq. 3.1}$$

To determine the specific surface area, Eq. 3.1 is linearized to calculate the volume of a monolayer (V_m) and the BET constant (C). The BET specific surface area, S_{BET} (m^2 g^{-1}) is then determined by Eq. 3.2, where m (g) is the mass of the sample, A (m^2) is the area occupied by an adsorbed molecule, N is Avogadro's constant, and V_M (m^3·mol^{-1}) is the molar volume.

$$S_{BET} = \frac{NAV_m 10^{-20}}{mV_M} \qquad \textit{Eq. 3.2}$$

Furthermore, the textural characterization of the materials was performed in the Quantachrome Instruments NOVA 4200e model. The samples were degassed following the heating program detailed in Figure 3.1.

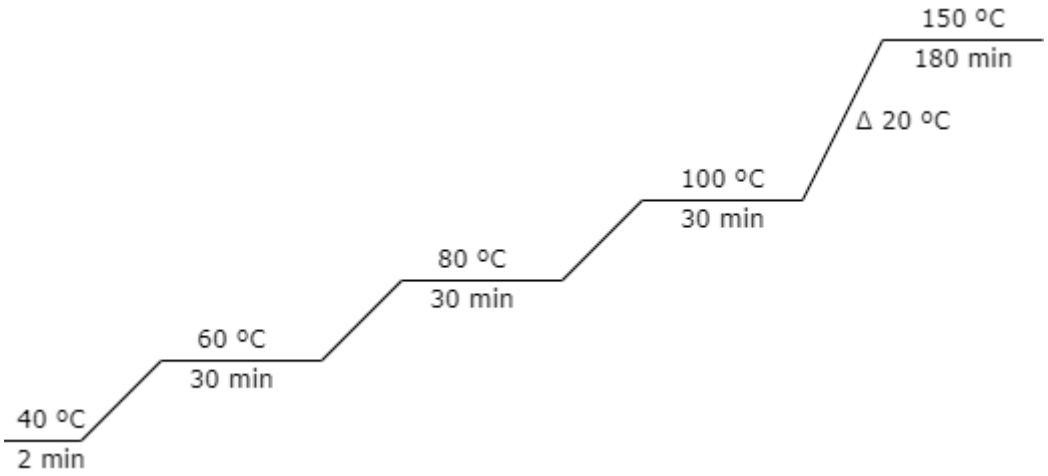

Figure 3.1: Degassing temperature program used in this work.

After cooling down to room temperature, the samples went through N_2 adsorption/desorption at -196 ºC.

3.2.3 Inductively Coupled Plasma Optical Emission Spectroscopy, ICP-OES

This method was used to analyse the amount of phosphorus in the samples. ICP-OES requires the conversion of a liquid into an aerosol of thin droplets via nebulization[77]. This aerosol is introduced into the plasma core via an argon flow, and thereby, if the sample is a solid material, an acid digestion must be employed to convert the solids to liquids[77].

Consequently, the samples were digested in a START D Microwave Digestion System using 10 mL of 65 % HNO_3 and 40 mL of ultrapure water, at 200 ºC for 15 min. Furthermore, the ICP analysis proceeded using an iCAP 7400 ICP-OES Analyzer. The analysis was carried out at 45 ºC, with a sample injection volume of 10 mL. The calibration curve was determined using the ICP multielement standard solution supplied by Merck, by preparing concentrations ranging from 5 to 10 000 ppb, and it can be found in Figure A.1, present in Appendix A.1.

3.2.4 Elemental Analysis, Micro and Oxycube

The oxygen content was determined via elemental analysis done in the Elementar Oxy Cube, which provides matrix-independent, high precision oxygen analysis. To perform the analysis, 1.5–2 mg of sample were weighted in a highly accurate Mettler M3 TG50 scale.

The Elementar Vario Micro El Cube equipment was used to analyze the amount of sulfur, carbon, nitrogen, and hydrogen in a sample, providing high precision elemental analysis. Moreover, to

perform the analysis, 1.5–2 mg of sample were weighted in a highly accurate Mettler M3 TG50 scale.

In both cases, the results were calculated by doing a three-point average of the individual results.

3.2.5 X-Ray Photoelectron Spectroscopy, XPS

XPS was used to characterize the composition, electronic state and the type of surface functional groups present on the samples. The analysis was performed in a Kratos AXIS ultra HAS, with VISION software for data acquisition and, for data analysis CasaXPS software was used. The analysis was performed using a monochromatic Al Ka X-Ray source, 1486.7 eV, at 15 kV, in Fixed Analyzer Transmission mode with a pass energy of 40 eV for the regions of interest and 80 eV for the survey. The spectra were fitted externally using previously described approaches and the type of species present were assigned based on the values of binding energy (BE) published in the literature. The energy scale of the spectrometer was correctly calibrated using a C1s peak which was placed at BE=284.5 eV, which was followed by a corresponding linear correction to the BE scale.

3.2.6 Scanning Electron Microscopy and Energy Dispersive X-ray Spectroscopy, SEM / EDS

The SEM / EDS analysis was performed to assess the homogeneity of the bulk composition of the materials as well as their morphology. It was done using a High resolution (Schottky) Environmental Scanning Electron Microscope with X-Ray Microanalysis and Electron Backscattered Diffraction analysis EDAX Genesis X4M. Samples were coated with an Au/Pd thin film, by sputtering, using the SPI Module Sputter Coater equipment. They were coated for 80 seconds with a 15 mA current, to enhance the material conductivity. The analysis was performed in *Centro de Materiais da Universidade do Porto* (CEMUP) within the campus of the University of Porto.

3.3 Catalytic performance

To assert the performance of the catalysts, fructose dehydration to HMF was chosen as a model reaction. The substrate was made with a 0.5 wt.% fructose solution in ultrapure water. The reaction was held in a batch Parr-type reactor equipped with a heating mantle and magnetic stirring. The prepared materials were tested at 180 °C for 2 hours using 3 bar of CO_2 initial pressure and continuous stirring at 600 rpm.

The reaction set-up was prepared by first introducing 40 mL of substrate along with 80 mg of catalysts. Afterwards, a magnetic stirrer is inserted in the reactor before it is closed. Once the substrate, the catalyst and the stirrer are in the reactor, and it is properly closed, 3 bar of CO_2

are introduced to set the initial pressure for the reaction. Furthermore, the reactor was placed in the heating mantle with a thermocouple inserted in it to measure the temperature. Finally, the heating was turned on and set at 180 °C, and, as soon as the temperature is reached, the magnetic stirrer is turned on at 600 rpm and the 2 hours of reaction begin.

Every 15 minutes, a sample of the reaction was collected to be analyzed in the high performance liquid chromatography (HPLC) equipment, with the first sample being at 0 minutes, *i.e.*, as soon as the reaction starts.

3.3.1 High Performance Liquid Chromatography, HPLC

In HPLC analysis, fructose was determined using a Refractive Index detector (RI) and HMF was analyzed using an Ultraviolet detector (UV).

The HPLC analyses were carried out using an Elite LaChrom HITACHI, equipped with a Hitachi L-2490 RI detector, a Hitachi L-2400 UV detector set at 254 nm wavelength, a Hitachi L-2200 auto-sampler and a Hitachi L-2130 pump. Furthermore, in the RI analysis, the separation took place in a Hichrim Altech OA – 1000 Organic Acid Column using a 0.005 mol·L^{-1} H_2SO_4 solution, as eluent, with a 0.5 mL·min^{-1} flow rate and an injection volume set at 40 µL. The UV analysis occurred using a Hydrosphere C18 column using 40 % v/v methanol in ultrapure water as eluent flowing at a 0.4 mL·min^{-1} flow rate and the injection volume was set at 10 µL.

The fructose and HMF calibration curves were both determined by HPLC RI and UV measurements, respectively, using stock solutions of the molecules with the following concentrations: 0.028 mol·L^{-1} , 0.022 mol·L^{-1}, 0.011 mol·L^{-1}, 0.0055 mol·L^{-1} and 0.0028 mol·L^{-1} for fructose and 0.022 mol·L^{-1}, 0.0176 mol·L^{-1}, 0.0088 mol·L^{-1}, 0.0044 mol·L^{-1}, 0.0022 mol·L^{-1} and 0.00088 mol·L^{-1}, for HMF. Each solution was made using ultrapure water. The calibration curves can be found in Figure A.2, present in Appendix A.2.

For each sample analyzed, the conversion of fructose was determined using Eq. 3.3, where n_x is the number of moles of fructose at *x* minutes of reaction and n_0 is the number of moles of fructose put into the reactor before heating up the reaction mixture. The selectivity to HMF was calculated as showed in Eq. 3.4, and the overall HMF yield was determined using Eq. 3.5.

$$Conversion\ of\ fructose\ (\%) = \frac{n_x}{n_0} \times 100 \qquad \textit{Eq. 3.3}$$

$$Selectivity\ to\ HMF\ (\%) = \frac{n\ HMF}{n\ Fructose\ Converted} \times 100 \qquad \textit{Eq. 3.4}$$

$$HMF\ Yield\ (\%) = \frac{Selectivity \times Conversion}{100} \qquad \textit{Eq. 3.5}$$

4 Results and discussion

In this Chapter, the results from the material characterization essays are detailed and analyzed. Furthermore, the Chapter will present and discuss the catalytic performance of the molasses-derived carbon catalysts in the fructose dehydration to HMF as a possible application of these materials.

4.1 Material bulk composition

As stated in Chapter 3, the prepared materials were subsequently functionalized using several treatments, providing each of these materials with unique bulk and surface chemistry and specific surface area. Table 4.1 depicts the bulk composition of the materials, obtained from EA.

Table 4.1: Bulk composition of the prepared carbon materials obtained from Elemental analysis (C, H, N, S) and oxy cube (O) in wt % of the material. Phosphorus was obtained from Inductive Coupled Plasma – Optical Emission Spectrometry.

Material	Element / wt.%					
	C[a]	H[a]	N[a]	S[a]	P[b]	O[a]
HTC	67.8	5.5	0.5	0	0	25.3
HTC_Carb	82.0	2.7	0.7	0	0	10.0
HTC_CO_2	82.0	2.0	0.7	0	0	11.2
HTC_Carb_O_2	34.3	1.7	0.3	0	0	23.7
HTC_H_3PO_4	68.5	5.5	0.5	0	0.9	19.7
HTC_H_3PO_4_Carb	82.5	2.9	0.7	0	0.4	10.1
HTC_Carb_H_2SO_4	80.7	2.7	0.6	1.5	0	12.7
HTC_Carb_HNO_3	80.2	1.9	1.1	0	0	10.6

[a]Measured by Elemental Analysis; [b]Measured by ICP-OES

Analyzing the data in Table 4.1, it becomes clear that material HTC_Carb_O_2 contains a substantial amount of impurities of unknown origin that were not analysed due to limited time of the project.

Moreover, it is possible to verify that once the material is carbonized, the carbon loading increases significantly, which was already expected. Furthermore, it is noticeable that, during carbonization, the materials lose some of their hydrogen and large amounts of oxygen groups, as shown by comparing HTC with HTC_Carb, where oxygen decreases from 25.3 % to 10 %, respectively. The amount of phosphorus dropped from 0.9 wt % present in HTC_H_3PO_4, to only 0.4 % present in HTC_H_3PO_4_Carb. In addition, when comparing carbon materials treated with

acids (H_3PO_4, H_2SO_4, and HNO_3) in Table 4.1, it can be confirmed that these treatments were successful in introducing heteroatoms such as: phosphorus in the case of HTC_H_3PO_4 and HTC_H_3PO_4_Carb; sulfur in HTC_Carb_H_2SO_4; and oxygen groups with a small amount of N (1.1 wt %) in HTC_Carb_HNO_3. The data in Table 4.1 shows that the materials functionalized by post-treatments showed similar amounts of oxygen to the carbonized sample; however, much higher amounts of oxygen were found in HTC_H_3PO_4, which was prepared by impregnation with 5 M H_3PO_4 for 24 hours under continuous stirring. This material has more oxygen content, likely due to it not being carbonized.

4.2 Material surface composition

To analyze the surface composition of the materials, XPS measurements were performed. XPS allows for the analysis of the overall surface chemistry of the materials. Table 4.2 summarizes the surface composition of the representative materials calculated based on the survey spectra given by XPS.

Table 4.2: Surface chemistry of the materials obtained from XPS.

Material	Element / wt.%				
	C	N	O	P	S
HTC	76.7	0.5	22.1	0	0.7
HTC_Carb_H_2SO_4	77.8	0	21	0	1.2
HTC_Carb_HNO_3	81.3	0.4	18.3	0	0
HTC_H_3PO_4_Carb	84.4	0	15.3	0.3	0

Comparing the results from surface and bulk analyses gathered in Table 4.2 and Table 4.1, respectively, it is possible to understand the dispersion of different elements in the samples. The reference material, HTC, shows small amounts of sulfur on its surface in XPS analysis; on the other hand, regarding bulk composition, only trace amounts of sulfur (< 0.1 %) have been measured. Nevertheless, the materials show similar composition on their surface as they do in the bulk, meaning that the elements were homogeneously distributed in these materials.

However, analyzing the oxygen content of the functionalized samples, the distribution is not homogeneous, as the material that went through post-synthesis functionalization has a higher oxygen wt.% on the surface than in the bulk, for example, HTC_Carb_HNO_3 records 10 % oxygen in the bulk whereas on the surface that value is 18.3 %. This means that most of the oxygen is in fact on the surface of these materials.

Furthermore, XPS analysis provides insight into the types of surface groups and the electronic state of the elements present on the surface of the materials. Using the CasaXPS software, the

spectra peaks of representative samples were deconvoluted externally. An example of the deconvoluted C1s, N1s high resolution spectrum and a high resolution XPS region of S2p spectra for the material HTC are present in Figure 4.1a, b, and c respectively. The remaining spectra can be found in Figure B.1 in Appendix B.1.

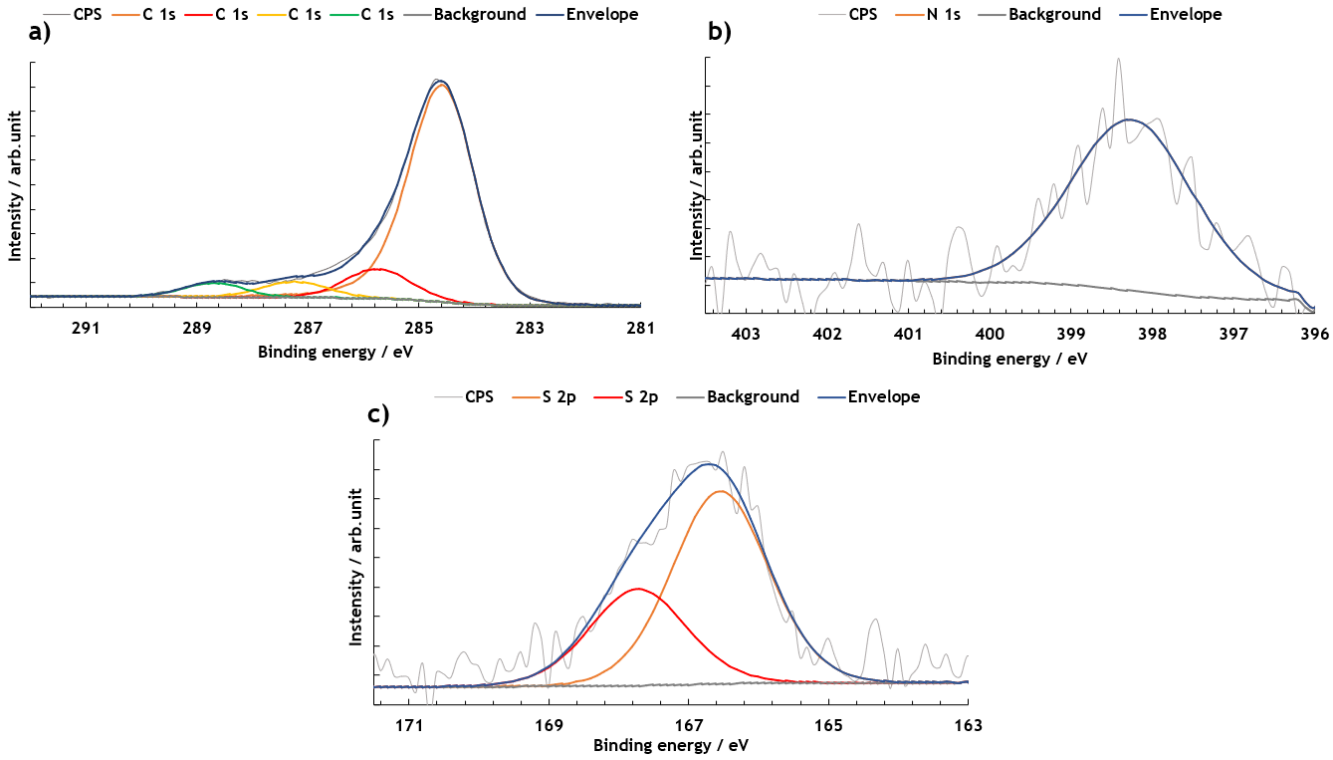

Figure 4.1: XPS of a) C1s region corresponding with the fitting of different carbon species, b) N1s region corresponding with the fitting of a nitrogen species, and c) S2p region showing typical spin-orbit splitting of S2p doublet $2p_{3/2}$ and $2p_{1/2}$ of material HTC.

The high-resolution C1s peaks for all the samples was centered at 284.5 eV with a tail towards higher binding energy, which is possible to verify in Figure 4.1a

Analyzing the C1s spectra depicted in Figure 4.1a, 4 distinct peaks can be identified for material HTC, with binding energies of 284.5 eV, 285.7 eV, 287.2 eV and 288.7 eV. The peak at 284.5 eV was assigned to graphitic carbon and corresponds to 80 % of the total carbon species, while the peak at BE = 285.7 eV was ascribed to phenolic carbon and it makes up 10.2 % of the total carbon species. Moreover, the peak at 287.2 eV corresponds to carbonylic carbon and amounts to 5.4 % of relative concentration, the last peak, which is the smallest peak, corresponds to 4.4 % of total carbon and has a binding energy of 288.7 eV and it was assigned to carboxylic carbon. Furthermore, Figure 4.1b, presents the nitrogen spectra of HTC, which as one peak corresponding to 100 % of the nitrogen present on the surface of the material and it is at a binding energy of 397.8 eV, which was assigned to nitride. This result makes sense as there were some nitrides in the molasses sample provided. Finally, Figure 4.1c depicts the S2p spectra of HTC, characterized by the spin-orbit splitting of the S2p doublet. The two peaks have a

binding energy of 166 eV and 167.2 eV, and were assigned to sulfoxide groups, corresponding to 100 % of the sulfur species in the material.

The remaining of the spectra for the other representative materials can be found in Appendix B.1.

Even though the C1s spectrum for HTC presents 4 individual peaks, the remaining materials present 5 peaks. The materials HTC_Carb_HNO_3, HTC_Carb_H_2SO_4, and HTC_H_3PO_4_Carb all present an intense peak at 284.5 eV, assigned to graphitic carbon, corresponding to the 83.5 %, 80.1 % and 79.5 %, respectively, of the total amount of carbon in the materials. Furthermore, these three materials show a broad, low intensity peak at 290 – 290.4 eV which was assigned to π-π^* transitions characteristic of pure graphitic samples. These peaks correspond to *ca.* 1 % of total carbon for all the samples. Moreover, HTC_Carb_HNO_3, HTC_Carb_H_2SO_4, and HTC_H_3PO_4_Carb have three peaks at 285.8 – 286 eV, 287 - 287.3 eV, and 288.6 – 289 eV, which were assigned to phenolic, carbonyl and carboxyl functionalities, respectively. In addition, for material HTC_Carb_HNO_3, phenolic functionalities corresponded to 2.9 % of total carbon, carbonyl to 9.5 % and carboxyl to 3.5 %. For HTC_Carb_H_2SO_4, these functionalities corresponded to 9.5 %, 5.1 % and 4.1 %, respectively. Finally, in HTC_H_3PO_4_Carb, the phenolic, carbonyl and carboxy functionalities correspond to 11.3 %, 4.5 % and 3.4 % of total carbon, respectively.

From these results, it is possible to verify that for the material treated with HNO_3, the phenolic relative concentration is lower than for other materials, while the carbonyl groups are present in a higher quantity. This could be explained by the liquid oxidation treatment made on the material, which seems to have increased carbonyl groups.

Regarding the N1s spectra of HTC_Carb_HNO_3, two peaks were recorded. At BE = 398.7 eV, the pyridinic functionality was assigned, corresponding to 34.6 % of total nitrogen. Furthermore, at 400.6 eV the other peak recorded was ascribed to a pyrrole functionality and it accounts for 65.4 % of total nitrogen in the sample. From these results, it is possible to very that the nitrides found in the parent material left the surface of the material, due to the carbonization and pyrrole and pyridinic groups were inserted by liquid phase oxidation with HNO_3.

Moreover, the S2p spectrum of HTC_Carb_H_2SO_4 shows two peaks at 168.2 eV and 169.4 eV, which were assigned to sulfonic surface groups and correspond to 100 % of total sulfur. The impregnation with H_2SO_4, was done with the objective of introducing sulfonic groups which are Brønsted acid functionalities.

Finally, the P2p spectrum of HTC_H_3PO_4_Carb shows two 2p peaks at 133.3 eV and 134.2 eV, which were ascribed to phosphate groups and correspond to 100 % of total phosphorus.

4.3 Analysis of the morphology, texture and bulk composition using SEM/EDS

SEM/EDS analyses are a useful tool to assert the homogeneity of the composition of the materials because they can reveal variations in the dispersion of various elements in different locations of the sample. Table 4.3 depicts the EDS analysis of different zones of materials HTC and HTC_H_3PO_4 marked in Figure 4.2 and Figure 4.3, respectively.

Table 4.3: The comparison of the composition obtained by SEM/EDS analyses of different zones in in samples HTC and HTC_H_3PO_4. For the positions of zones within HTC samples see Figure 4.2, and for the positions of zones in HTC_H_3PO_4 sample see Figure 4.3.

Catalyst	Zone	Element / wt.%					
		C	O	P	S	Ca	Si
HTC	Z1	66.6	29.5	0.2	0.5	0.4	2.8
	Z2	73.7	25.8	0	0	0	0.5
	Z3	50.9	38.3	0	0.4	10.5	0
HTC_H_3PO_4	Z1	70.8	27.1	1.3	0	0.9	0
	Z2	72.4	26.5	0.6	0	0.5	0
	Z3	70.0	27.2	1.7	0	1.1	0
	Z4	74.7	24.8	0.2	0	0.3	0

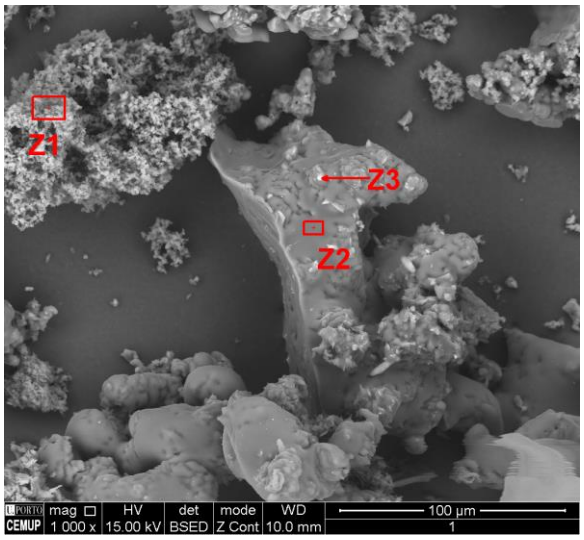

Figure 4.2: SEM image of HTC with the marked zones of analysis Z1, Z2 and Z3.

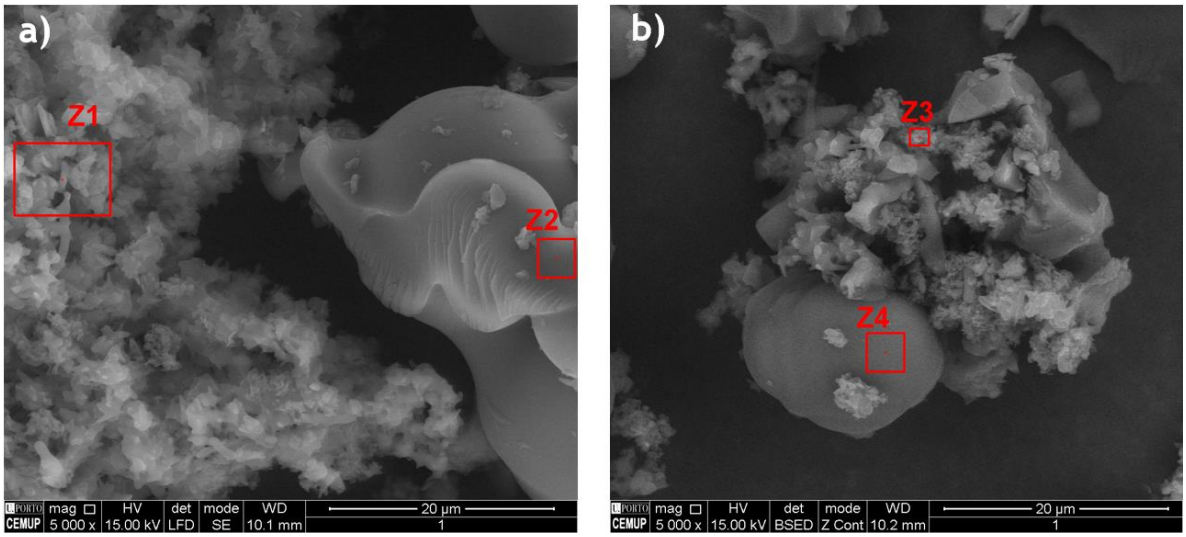

Figure 4.3: SEM images of HTC_H_3PO_4 where a) shows zones Z1 and Z2 and b) shows zones Z3 and Z4.

Figure 4.2 depicts the zones of the HTC material that were analyzed regarding bulk composition of the samples. From the data showed in Table 4.3 it can be concluded that the composition of both materials was not fully uniform and there were clearly some variations of the concentrations of different elements depending on the analyzed zone. For example, comparing the concentration of carbon in zones 1-3, it is clear that Z2 shows a much higher amount of carbon than zones Z1 and Z3. In addition, Z3 is richer in oxygen than Z1 and Z2. Moreover, large amounts of Ca were measured in Z3 along with some Si impurities in Z1. These outliers may be due to contamination during material preparation or may have already been present in the molasses sample provided. Furthermore, sulfur was found in similar concentration in Z1 and Z3; however, no traces of this element were found in Z2.

Figure 4.3 shows the zones of HTC_H_3PO_4. The data detailed in Table 4.3, shows that, in comparison with the HTC material, HTC_H_3PO_4, is more uniform in its bulk composition. However, it is not fully homogeneous, as it can be concluded from the data. Regarding carbon concentrations, zones Z2 and Z4 show a slightly higher concentration than zones Z1 and Z3. Moreover, the zones with higher carbon concentration, Z2 and Z4, show lower oxygen concentrations than zones Z1 and Z3. In addition, it is clear from the data that zones Z1 and Z3 have higher concentrations of phosphorus, while in zones Z2 and Z4 these concentrations are lower. This material also shows some more dispersed Ca impurities than the HTC material, though in lower concentrations. The lower impurity content in material HTC_H_3PO_4 may be due to the fact that some of the inorganic impurities could have been washed off during the treatment of the material in the phosphoric acid. Analyzing these concentrations, it becomes clear that zones Z1 and Z3 are quite similar in bulk composition as are zones Z2 and Z4. Figure 4.3 also shows that, along with the composition, zones Z1 and Z3 have similar morphology, with smaller and more agglomerated particles, and zones Z2 and Z4, while also being similar to each other, show bigger sized particles.

Comparison of the morphology of the materials HTC and HTC_H_3PO_4 will be made using Figure 4.4.

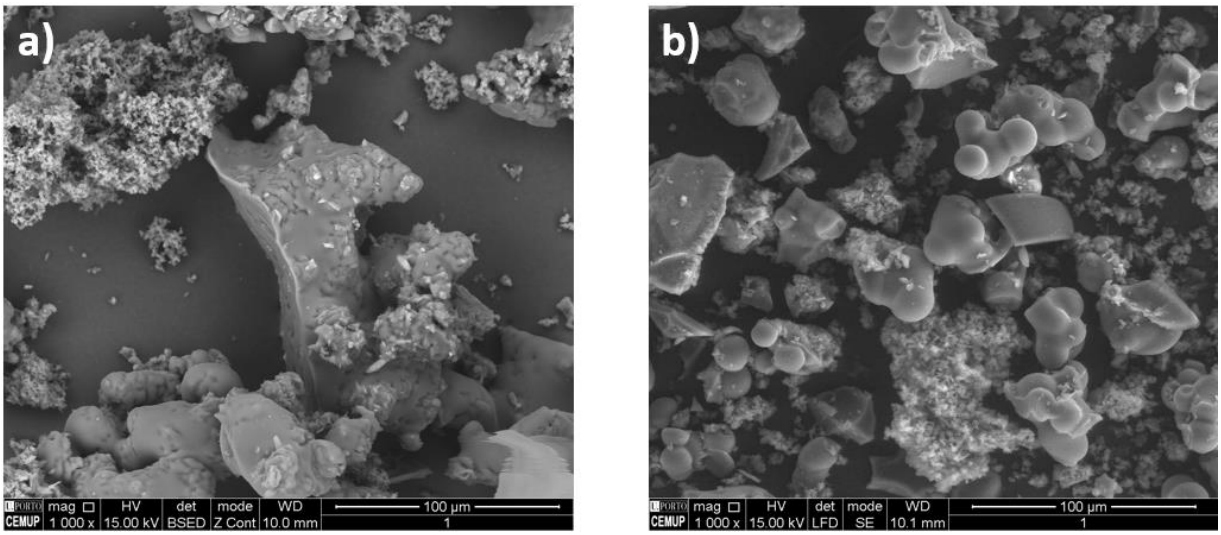

Figure 4.4: SEM images with 1000x ampliation of materials a) HTC and b) HTC_H_3PO_4.

Analyzing Figure 4.4., it is visible that both materials are highly heterogeneous. Furthermore, material HTC does not show any well-defined shaped particle but, overall, it has bigger particles than HTC_H_3PO_4. Despite, in accordance with material HTC, the particles of HTC_H_3PO_4 being overall not uniform and not well defined, this material also shows some well-defined spherical particles.

4.4 Material stability to oxidation

To assess material stability against oxidation, thermogravimetric analysis was performed in an air flow. This analysis was performed to verify if molasses-based carbon materials can be applied in high temperature reactions or in oxidative gas phase reactions at elevated temperatures.

The first derivatives of the mass loss in temperature were calculated (DTG) in order to obtain the temperature at which the maximum weight loss occurred in all of the samples, called T_{max}. The higher the T_{max}, the more stable the material is in the oxidative environment. Figure 4.5 depicts the TG curve recorded for the HTC sample, under air atmosphere, as well as the first derivative of this curve. The results for other materials are gathered in Figure B.2 in Appendix B.2.

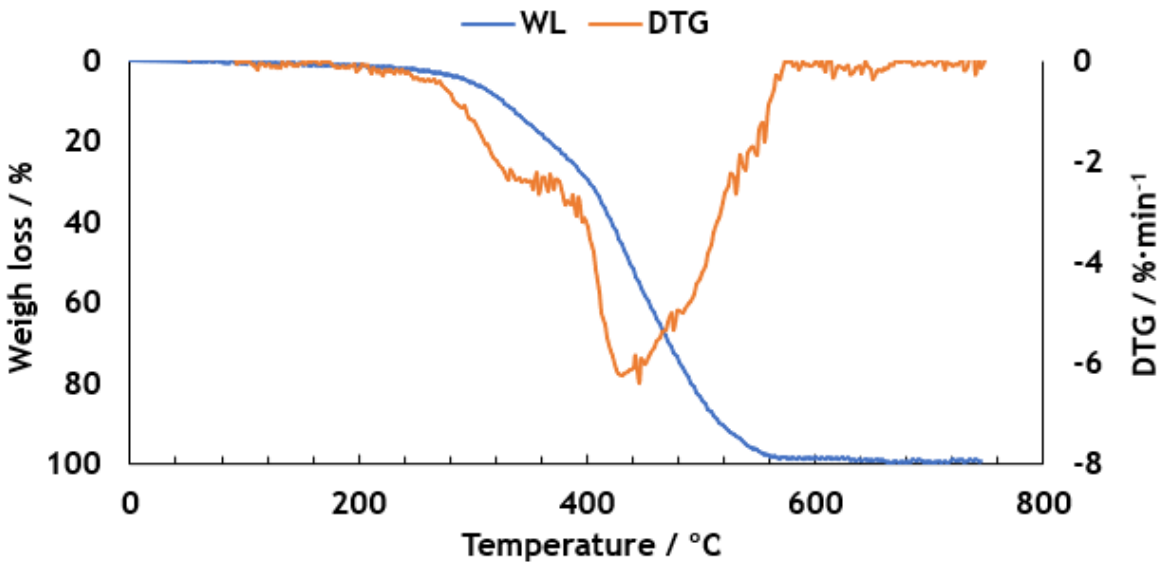

Figure 4.5: TG and DTG of HTC sample.

From Figure 4.5 it is possible to observe that the material starts to burn and lose mass at around 300 °C and that, at *ca.*, 600 °C, most of the material has been effectively burned off, and at the end of the heating programme, there was a residue of 0.9 %. This residue can be assumed as ashes, even though the procedure of the measurement of the ash content in carbons is different to the one applied in this work. Examining the DTG of this material, it is possible to notice a sharp peak at around 430 °C, which indicates the T_{max}. The T_{max} values obtained for all of the samples studied here are compared in Table 4.4.

Table 4.4: T_{max} of each sample obtained by the 1st derivative of the TG curve

Sample	$T_{máx}$ / °C
HTC	430
HTC_Carb	520
HTC_CO_2	550
HTC_Carb_O_2	400
HTC_H_3PO_4	510
HTC_H_3PO_4_Carb	580
HTC_Carb_H_2SO_4	550
HTC_Carb_HNO_3	540

First, material HTC_Carb_O_2 appears to be an outlier, since it would make sense that it had a higher T_{max} than the HTC material, because of the treatments this material underwent. Unfortunately, as was demonstrated by other characterization techniques (Elemental analysis), this sample contains a large amount of impurities (ash), thus it cannot be compared to the rest of the materials, and it will not be considered in the remaining part of the results of this work.

Analyzing the data in Table 4.4, it is possible to infer which treatments rendered the materials that are more stable against oxidation. Focusing on HTC and HTC_Carb, it is visible that the value for T_{max} increases along these samples, which suggests that carbonized material is more stable than the non-carbonized material, which is likely due to the loss of less stable functional groups via carbonization. Moreover, the higher the temperature of the carbonization, the higher the stability of the material, since HTC_Carb was carbonized at 600 ºC and HTC_CO_2 was carbonized at 750 ºC. Of course, to effectively compare these temperatures, both carbonizations would have to have been performed under the same atmosphere. However, the effects of the treatment atmosphere on the stability of the carbon materials can be assumed to be smaller than the effect of the temperature of the treatments.

Now comparing materials HTC and HTC_H_3PO_4, the latter showed a much higher T_{max}, entailing that the treatment with H_3PO_4 increased the material's stability against oxidation, which is well reported in the literature[78]. Furthermore, comparing the materials HTC_Carb, HTC_H_3PO_4_Carb, HTC_Carb_H_2SO_4 and HTC_Carb_HNO_3, it is also possible to draw the same conclusion, that is, the treatments performed with acids increased the material's resistance to oxidation, possibly due to the washing of impurities present in the molasses that could catalyze the oxidation reaction.

4.5 BET surface area

The surface area of the materials was determined by N_2 adsorption / desorption at -196 ºC. The obtained results are summarized in Table 4.5.

Table 4.5: BET surface area of the materials measured by N_2 adsorption / desorption at -196 ºC.

Sample	BET surface area / $m^2 \cdot g^{-1}$
HTC	19
HTC_Carb	58
HTC_CO_2	354
HTC_H_3PO_4	88
HTC_H_3PO_4_Carb	15
HTC_Carb_H_2SO_4	18
HTC_Carb_HNO_3	34

By analyzing Table 4.5, it can be verified that the surface area of the material increases slightly with carbonization in N_2, which is noticeable when comparing materials HTC and HTC_Carb. Furthermore, material HTC_CO_2 presented the highest surface area out of all the materials, meaning that carbonizations in a CO_2 atmosphere increase the surface area. This surface area increase is owed to the fact that CO_2 is a weak oxidizing agent that effectively burns the

material, generating porosity[79]. Furthermore, it appears that the treatment with acids slightly lowers the surface area of the materials except for the treatment with H_3PO_4. From the literature, it would make sense that surface area increases with impregnation in H_3PO_4[80]; although, that increase should have been after the material got carbonized[80]. However, it is clear from the data in Table 4.5, that the surface area decreased after carbonization, which goes against what was expected.

4.6 Catalytic performance

The catalytic performance of the materials was tested in fructose dehydration to HMF in water using a batch reactor. The testing was carried out during 2 hours of reaction time at 180 ºC, with an initial pressure of 3 bar of CO_2 and continuous stirring set at 600 rpm. A total of 9 samples were taken from the reaction mixture during the testing, in time spans of 15 min. Time zero was assigned when the reaction temperature was reached.

Since this is a reaction where the substrate is fructose and the main product is HMF, what is expected to happen is that, throughout the reaction, fructose is consumed while HMF is formed, and the cumulate conversion, $X_{fructose}$, continuously increases. Figure 4.6 depicts the evolution of the reaction with time.

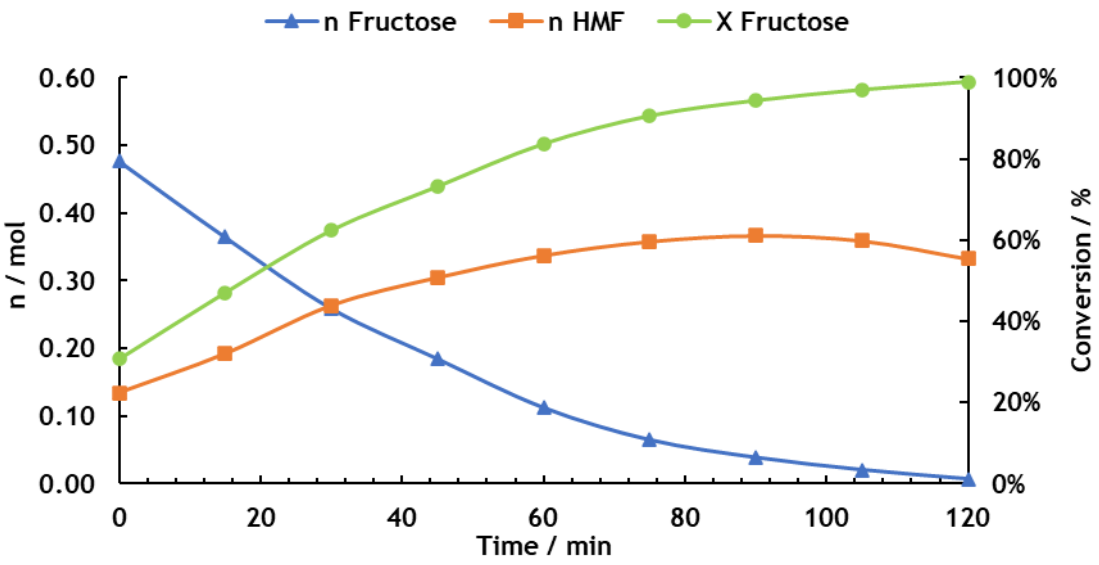

Figure 4.6: Fructose dehydration to HMF, reaction evolution.

Analyzing Figure 4.6, it is possible to verify that the conversion increases with reaction time, reaching almost 100 %. Moreover, it can also be noticed that the moles of fructose decrease while the moles of HMF increase with reaction time.

The highest yield of HMF was registered at 90 min reaction time, and thus, the catalytic performance of all the catalysts tested was compared at 90 min reaction time. Figure 4.7

depicts the yield, selectivity, and conversion at 90 minutes of reaction for the blank reaction (without any catalysts), the HTC material, which is the reference material in this work, and the remaining carbonized materials, without any acid treatments.

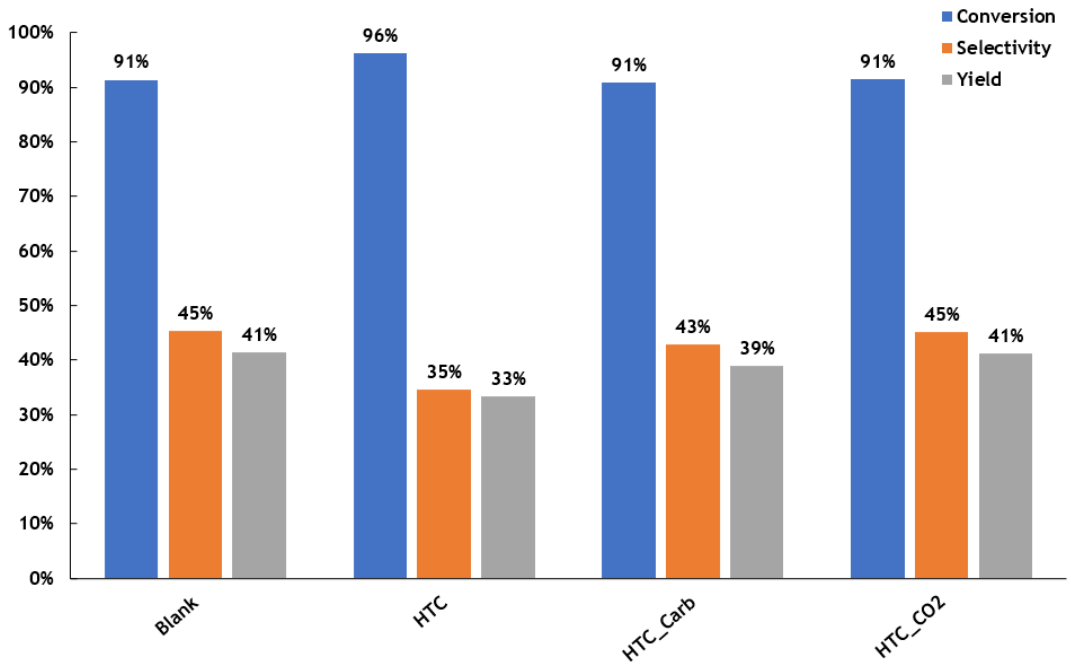

Figure 4.7: Catalytic performance of the carbonized materials

From the bar chart present in Figure 4.7, it is possible to compare the performance of material HTC with HTC_Carb. It is clear that carbonization removed some surface groups from the surface of HTC, leading to a decrease in fructose conversion from 96 %, recorded for HTC, to 91 %, recorded for HTC_Carb. Interestingly enough, the selectivity of HMF increased for HTC_Carb, from 35 % to 43 %.

Moreover, it is visible that the reaction performance from the blank is as high as the performance of the material with the highest surface area, namely HTC_CO_2. What this result seems to suggest is that, for the reaction in study, fructose dehydration to HMF, surface area alone does not have a withstanding influence.

To complement the study, the influence of catalysts containing Brønsted acid sites in the form of phenol and carboxyl groups, sulphonic groups and phosphate functionalities was assessed. Figure 4.8 entails the comparison of reaction performances between the carbonized materials that have been functionalized with Brønsted acid sites. In Figure 4.8, HTC_Carb material will be considered the reference material, as it is the parent material for the other samples.

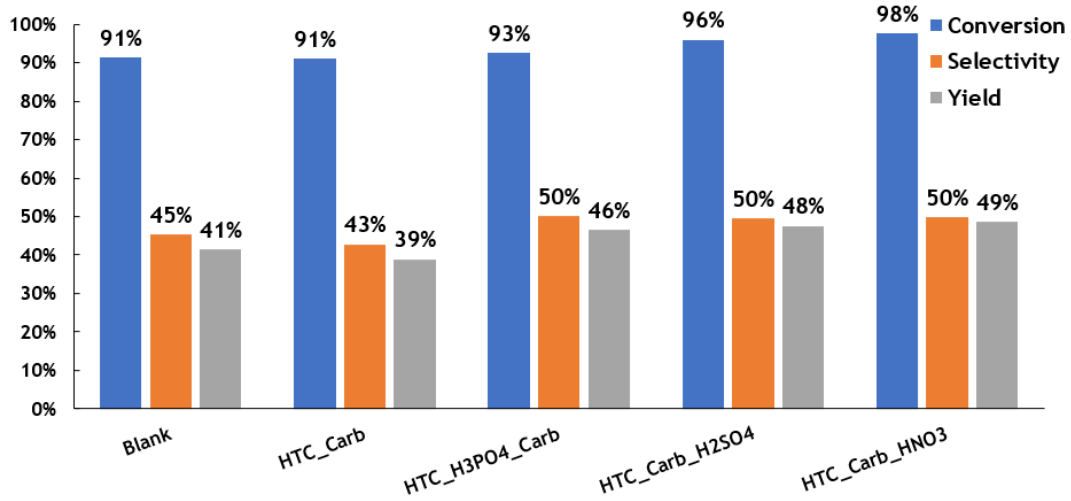

Figure 4.8: Catalytic performance of the carbonized materials treated in acid.

From Figure 4.8, one can infer that the treatments with acid influence the performance of the reaction positively, garnering higher yields and selectivities than the non-treated materials. These results are likely due to the introduction of Brønsted acid sites on the material surface, namely, sulphonic groups in HTC_Carb_H_2SO_4, and phenolic and carboxylic groups on all three materials. Furthermore, in Figure 4.8, it is clear that material HTC_Carb_HNO_3, obtained the highest fructose conversion, and HFM yield out of all the samples, with values corresponding to 98 % and 49 %, respectively. In addition, all three functionalized materials recorded 50 % of HMF selectivity, which is higher than the reference. Finally, all three functionalized materials recorded higher fructose conversion, HMF yield and HMF selectivity than the material with the highest surface area, HTC_CO_2, when comparing Figure 4.8 with Figure 4.7. This leads to the conclusion that in the reaction of interest, surface chemistry affects the catalytic performance more positively than surface area.

Finally, Figure 4.9 presents the box chart where a comparison is made between the blank and the HTC material, and the only material that was treated with acid without any carbonization.

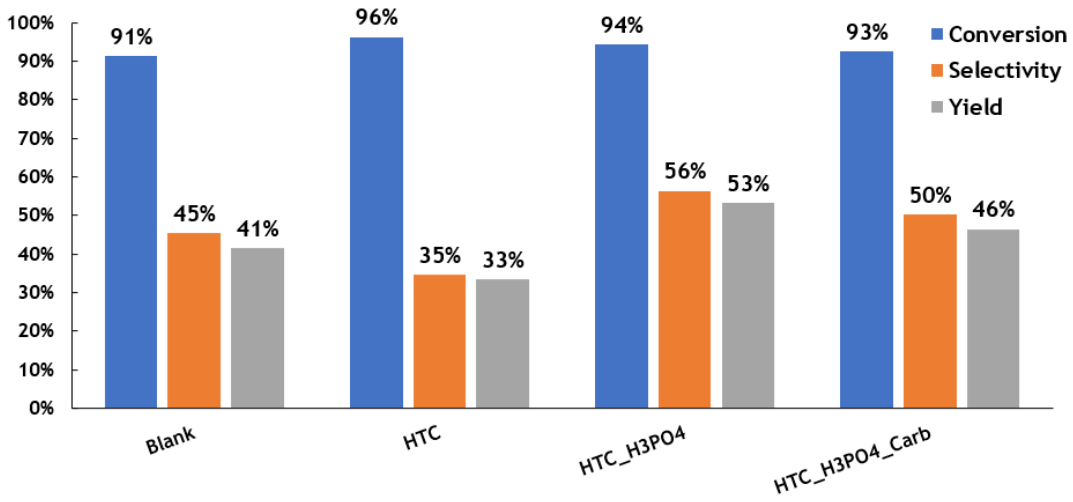

Figure 4.9: Catalytic performance of the materials treated with H_3PO_4, before and after carbonization.

Analyzing the data from Figure 4.9, it is possible to verify clearly which is the best catalyst. Material HTC_ H_3PO_4 recorder higher fructose conversion, HMF yield and HMF selectivity than material HTC_ H_3PO_4_Carb. The reason for this difference could be explained by the fact that during carbonization some phosphorus left the material, as it was showed by the ICP analysis (see Table 4.1). The difference in phosphorus concentration is likely to the loss of surface groups during carbonization, which means that the carbonized material would have less surface phosphorus functionalities than the non-carbonized material (HTC_ H_3PO_4). As seen from the data in Figure 4.9 this led to an increase in performance in all three parameters (fructose conversion, HMF selectivity and HMF yield). It is underlined that the material HTC_ H_3PO_4, underwent a thorough washing to desorb the phosphoric acid that it had adsorbed during immersion. Thus, this result cannot be owed to homogenous catalysis catalyzed by H_3PO_4, as after the washing the pH of the filtrate was 7, meaning that all the phosphoric acid had been desorbed during washing.

5 Conclusion

The last several decades recorded a large population increase, and the amount of solid waste generated followed the same trend. In the sugar industry, the most generated by-product is sugar cane molasses, which is a substance from which no more sugar can be extracted by crystallization. The focus of this project was to create carbon materials through hydrothermal carbonization with the objective of valorizing molasses, thus increasing its market value, while taking steps towards a circular economy. In this work, the carbon materials produced from molasses were applied as catalysts in the fructose dehydration to 5-hydroxymethylfurfural (HMF). The prepared carbon materials were functionalized with Brønsted acid active sites, namely, oxygen, phosphorus, and sulfur surface groups.

In this work, an optimization of the HTC process was carried out, by testing different water to molasses weight ratios (1:1, 1:2, 2:1) and different carbonization temperatures (170 ºC, 180 ºC, 190 ºC). For further functionalizations, the material with a 1:1 water to molasses weight ratio carbonized at 180 ºC was selected as a starting point. The material was functionalized with Brønsted acid sites by applying several procedures such as: high-temperature carbonization, in N_2 and CO_2, treatment under 5 % (v/v) O_2/N_2, and impregnation with H_2SO_4 and H_3PO_4, and liquid-phase oxidation with HNO_3.

Throughout the work, these materials were characterized by elemental analysis, X-ray photoelectron spectroscopy, inductive coupled plasma – optical emission spectroscopy, scanning electron microscopy/energy dispersive x-ray spectroscopy, thermogravimetric analysis and N_2 adsorption/desorption at -196 ºC.

From the characterizations made, it was concluded that materials significantly increase their carbon content by carbonization. On the other hand, some functional groups containing hydrogen, oxygen and phosphorus can leave the surface of the materials, while some hydrogen, oxygen, and phosphorus groups leave the surface of the materials during carbonization. Furthermore, by comparing the bulk composition with the surface composition, it was clear that the materials were mostly uniform, although the materials functionalized with Brønsted acid sites recorded higher oxygen percentage on the surface than in the bulk, showing that most of the oxygen is present on the surface of these materials due to post treatment functionalization. XPS analysis showed the presence of nitride on the surface of the reference hydrochar (made by HTC in 1:1 water to molasses weight ratio at 180 ºC), as well as the presence of sulfoxide. This entails that the original molasses sample had these groups in its composition. Moreover, it showed the presence of sulfonic surface functionalities on the material treated with H_2SO_4, phosphate functionalities on the surface of the material treated

with H_3PO_4, and pyrrole and pyridine functionalities on the surface of the material treated in HNO_3. Finally, all the materials had graphitic, phenolic, carbonyl and carboxylic carbon groups, and, in addition, the functionalized materials also showed a low intensity peak assigned to π-π* transitions.

Regarding material stability to oxidation, it was concluded that, in addition to carbonized materials becoming more stable than their non-carbonized counterparts, the acid treatments done in this work provide the materials with higher stability to oxidation, likely due to the removal of impurities from molasses that were catalyzing the oxidation of HTC material. The material that presented itself as the most stable was HTC_H_3PO_4_Carb, meaning that the treatment with phosphoric acid develops more stable materials when it comes to oxidation, which has been known to happen in H_3PO_4 treatments.

The results concerning the BET surface area show that the material carbonized in CO_2 flow named HTC_CO_2 obtained the highest BET specific surface area, 354 $m^2 \cdot g^{-1}$, which indicates that high-temperature treatment in CO_2 appears to be a good method to introduce pores into carbon materials.

The catalytic performance of the materials was analyzed and from the results gathered, it was possible to verify that the materials with the higher surface area had a poor reaction performance, leading to the conclusion that in the reaction of interest, BET surface area does not have a significant effect. Moreover, BET surface area affects the reactions in the gas-phase more and there is plenty of reports in the literature describing great catalytic performance of hydrochars from biomass with very low surface area, but rich surface chemistry. Furthermore, it was possible to determine from the recorded data that the acid treatments significantly increased the yield and selectivity of HMF, likely due to the fact that these materials had Brønsted acid functionalities on their surface, which was confirmed by the XPS analysis.

Finally, the catalyst functionalized with phosphoric acid, HTC_H_3PO_4, was found to be the best performing material, achieving an HMF yield of 53 % and 56 % of selectivity to HMF.

In addition, future interesting and important work would be the optimization of the hydrothermal carbonization process. Optimizing the HTC reaction conditions, such as water to molasses ratio, HTC temperature and duration of the process, would lead to a better starting material that ultimately could lead to better final materials.

Furthermore, the results from this work showed that impregnation was not the most effective way to functionalize the hydrochars, since the percentages of heteroatoms reported in the data obtained were very low. Thus, the study of other methods to functionalize the hydrochars other than impregnation would be a very interesting next step.

In addition, it would be interesting to perform the catalysts recyclability tests in the fructose dehydration and how long it would take for them to deactivate, as well as the overall reproductivity of this work.

Finally, it would be very interesting to explore other means of adding value to molasses other than its use in catalysis. Exploring the preparation of highly microporous materials for adsorbents or the introduction of nitrogen functionalities for wastewater treatment would also be interesting next steps toward the valorization of molasses.

6 Assessment of the work done

6.1 Objectives Achieved

In this work, the main objective was to use molasses as raw material to produce carbon materials, thus increasing its market value, while additionally using a substance that is often viewed as a waste; instead, this creates a material with a high value, which is a great way of valorizing and helping the environment by creating a circular economy.

Furthermore, the obtained materials were applied as catalysts in fructose dehydration to 5-hydroxymethylfurfural (HMF). The active sites were introduced on the surface of the catalysts using various techniques.

As far as the first objective goes, the materials developed regardless of their reaction performance increase the value of molasses and these hydrochars can be used for other interesting applications apart from catalysis. Furthermore, a method was developed to convert molasses into good quality carbon materials that were active catalysts in conversion of fructose to HMF in water. Hence, it can be considered that the second objective was successfully achieved.

6.2 Final Assessment

This project appears to be a very important one for RAR in a financial standpoint since it is able to prove that molasses can be viewed as a product of higher value than waste and that can be commercialized by the company to increase its earnings, while reducing waste.

Furthermore, with this project, the objective of producing HMF from 100 % molasses becomes one step closer, and surely, with more work and research, in the near future, HMF production from 100 % upcycled molasses will become a reality.

From a personal point of view, this work has been a real growth experience, and has made the author realize the somewhat beauty of laboratory work. Of course, knowing that the work that is being done can, in some way, shape or form, help the environment, has been a very fulfilling experience.

7 References

1. Silpa K, Yao L, Bhada-Tata P. *What a Waste 2.0: A Global Snapshot of Solid Waste Management to 2050*.; 2019. Accessed March 12, 2022.
2. Shah A V., Srivastava VK, Mohanty SS, Varjani S. Municipal solid waste as a sustainable resource for energy production: state-of-the-art review. *J Environ Chem Eng*. 2021;9(4):105717. doi:10.1016/J.JECE.2021.105717
3. The Sugar Association. What Is molasses: all you need to know. Published 2020. Accessed March 12, 2022. https://www.sugar.org/blog/molasses-all-you-need-to-know/
4. ISO. By-Products. Published 2020. Accessed March 8, 2022. https://www.isosugar.org/sugarsector/by-products
5. Palmonari A, Cavallini D, Sniffen CJ, et al. Short communication: characterization of molasses chemical composition. *J Dairy Sci*. 2020;103(7):6244-6249. doi:10.3168/jds.2019-17644
6. Sugarcane.org. Sugarcane. Green Energy: An A-to-Z Guide. doi:10.4135/9781412971850.n47
7. Valero-Romero MJ, García-Mateos FJ, Rodríguez-Mirasol J, Cordero T. Role of surface phosphorus complexes on the oxidation of porous carbons. *Fuel Process Technol*. 2017;157:116-126. doi:10.1016/j.fuproc.2016.11.014
8. Nguyen TLT, Gheewala SH, Garivait S. Full chain energy analysis of fuel ethanol from cane molasses in Thailand. *Appl Energy*. 2008;85(8):722-734. doi:10.1016/j.apenergy.2008.02.002
9. Clarke MA. SYRUPS. In: *Encyclopedia of Food Sciences and Nutrition*. Elsevier; 2003:5711-5717. doi:10.1016/b0-12-227055-x/01175-5
10. Jamir L, Kumar V, Kaur J, Kumar S, Singh H. Composition, valorization and therapeutical potential of molasses: a critical review. *Environ Technol Rev*. 2021;10(1):131-142. doi:10.1080/21622515.2021.1892203
11. Observatory of ecomomic O. Ethylene (HS: 290121) Product Trade, Exporters and Importers | OEC - The Observatory of Economic Complexity. Accessed March 7, 2022. https://oec.world/en/profile/hs92/molasses
12. IHS. *Molasses & Feed Ingredients Market Outlook*.; 2019. Accessed March 7, 2022. https://ihsmarkit.com/products/food-commodities-food-manufacturing-softs-molasses-feed-ingredients.html

13. Nikodinovic-Runic J, Guzik M, Kenny ST, Babu R, Werker A, O'Connor KE. Carbon-rich wastes as feedstocks for biodegradable polymer (polyhydroxyalkanoate) production using bacteria. In: *Advances in Applied Microbiology*. Vol 84. Academic Press Inc.; 2013:139-200. doi:10.1016/B978-0-12-407673-0.00004-7

14. KNOEMA. Production statistics - crops processed. Published 2017. Accessed March 8, 2022. https://knoema.com/FAOPRDSC2020/production-statistics-crops-crops-processed?tsId=1515900

15. WITS. Portugal Sugars; molasses, from sugar cane, resulting from the extraction or refining of sugar exports by country. Published 2019. Accessed March 8, 2022. https://wits.worldbank.org/trade/comtrade/en/country/PRT/year/2019/tradeflow/Exports/partner/ALL/product/170310#

16. Legrouri K, Khouya E, Ezzine M, et al. Production of activated carbon from a new precursor molasses by activation with sulphuric acid. *J Hazard Mater*. 2005;118(1-3):259-263. doi:10.1016/j.jhazmat.2004.11.004

17. Jeong SY, Lee JW. Hydrothermal treatment. In: *Pretreatment of Biomass: Processes and Technologies*. Elsevier; 2015:61-74. doi:10.1016/B978-0-12-800080-9.00005-0

18. Funke A, Ziegler F. Hydrothermal carbonization of biomass: A summary and discussion of chemical mechanisms for process engineering. *Biofuels, Bioprod Biorefining*. 2010;4(2):160-177. doi:10.1002/bbb.198

19. Nicolae SA, Au H, Modugno P, et al. Recent advances in hydrothermal carbonisation: from tailored carbon materials and biochemicals to applications and bioenergy. *Green Chem*. 2020;22(15):4747-4800. doi:10.1039/d0gc00998a

20. Figueiredo JL. Functionalization of porous carbons for catalytic applications. *J Mater Chem A*. 2013;1(33):9351-9364. doi:10.1039/c3ta10876g

21. Inagaki M, Toyoda M, Soneda Y, Morishita T. Nitrogen-doped carbon materials. *Carbon N Y*. 2018;132:104-140. doi:10.1016/j.carbon.2018.02.024

22. Kalijadis A, DorCevidć J, Trtić-Petrović T, et al. Preparation of boron-doped hydrothermal carbon from glucose for carbon paste electrode. *Carbon N Y*. 2015;95:42-50. doi:10.1016/j.carbon.2015.08.016

23. Clarke MA. SYRUPS. *Encycl Food Sci Nutr*. Published online 2003:5711-5717. doi:10.1016/B0-12-227055-X/01175-5

24. Pauline AL, Joseph K. Hydrothermal carbonization of organic wastes to carbonaceous solid fuel – a review of mechanisms and process parameters. *Fuel*. 2020;279:118472. doi:10.1016/j.fuel.2020.118472

25. Hu B, Wang K, Wu L, Yu SH, Antonietti M, Titirici MM. Engineering carbon materials from the hydrothermal carbonization process of biomass. *Adv Mater*. 2010;22(7):813-828. doi:10.1002/adma.200902812

26. Tombari E, Salvetti G, Ferrari C, Johari GP. Kinetics and thermodynamics of sucrose hydrolysis from real-time enthalpy and heat capacity measurements. *J Phys Chem B*. 2007;111(3):496-501. doi:10.1021/jp067061p

27. Dinjus E, Kruse A, Tröger N. Hydrothermal carbonization - influence of lignin in lignocelluloses. *Chem Eng Technol*. 2011;34(12):2037-2043. doi:10.1002/ceat.201100487

28. Titirici MM, White RJ, Falco C, Sevilla M. Black perspectives for a green future: hydrothermal carbons for environment protection and energy storage. *Energy Environ Sci*. 2012;5(5):6796-6822. doi:10.1039/C2EE21166A

29. Li L, Wang Y, Xu J, Flora JRV, Hoque S, Berge ND. Quantifying the sensitivity of feedstock properties and process conditions on hydrochar yield, carbon content, and energy content. *Bioresour Technol*. 2018;262:284-293. doi:10.1016/j.biortech.2018.04.066

30. Romero-Anaya AJ, Ouzzine M, Lillo-Ródenas MA, Linares-Solano A. Spherical carbons: synthesis, characterization and activation processes. *Carbon N Y*. 2014;68:296-307. doi:10.1016/j.carbon.2013.11.006

31. Mao H, Chen X, Huang R, et al. Fast preparation of carbon spheres from enzymatic hydrolysis lignin: Effects of hydrothermal carbonization conditions. *Sci Rep*. 2018;8(1):1-10. doi:10.1038/s41598-018-27777-4

32. Sevilla M, Fuertes AB. Chemical and structural properties of carbonaceous products obtained by hydrothermal carbonization of saccharides. *Chem – A Eur J*. 2009;15(16):4195-4203. doi:10.1002/CHEM.200802097

33. Foroutan R, Peighambardoust SJ, Peighambardoust SH, Pateiro M, Lorenzo JM. Adsorption of crystal violet dye using activated carbon of lemon wood and activated carbon/fe3 o4 magnetic nanocomposite from aqueous solutions: A kinetic, equilibrium and thermodynamic study. *Molecules*. 2021;26(8):1-19. doi:10.3390/molecules26082241

34. González-García P. Activated carbon from lignocellulosics precursors: A review of the synthesis methods, characterization techniques and applications. *Renew Sustain Energy Rev*. 2018;82:1393-1414. doi:10.1016/j.rser.2017.04.117

35. Balcerek M, Pielech-Przybylska K, Patelski P, Dziekońska-Kubczak U, Jusel T. Treatment with activated carbon and other adsorbents as an effective method for the removal of volatile compounds in agricultural distillates. *Food Addit Contam - Part A Chem Anal Control Expo Risk Assess*. 2017;34(5):714-727. doi:10.1080/19440049.2017.1284347

36. Xing BL, Guo H, Chen LJ, et al. Lignite-derived high surface area mesoporous activated carbons for electrochemical capacitors. *Fuel Process Technol*. 2015;138:734-742. doi:10.1016/j.fuproc.2015.07.017

37. Baig MM, Gul IH. Conversion of wheat husk to high surface area activated carbon for energy storage in high-performance supercapacitors. *Biomass and Bioenergy*. 2021;144:105909. doi:10.1016/j.biombioe.2020.105909

38. Serafin J, Ouzzine M, Cruz Junior OF, Sreńscek-Nazzal J. Preparation of low-cost activated carbons from amazonian nutshells for CO2 storage. *Biomass and Bioenergy*. 2021;144:105925. doi:10.1016/j.biombioe.2020.105925

39. Marsh H, Reinoso FR. *Activated Carbon*.; 2006. Accessed July 3, 2022.

40. Johnson C. Advances in pretreatment and clarification technologies. In: *Comprehensive Water Quality and Purification*. Vol 2. Elsevier Inc.; 2014:60-74. doi:10.1016/B978-0-12-382182-9.00029-3

41. Rodríguez-Reinoso F. Activated carbon andadsorption. In: *Encyclopedia of Materials: Science and Technology*. Elsevier; 2001:22-34. doi:10.1016/b0-08-043152-6/00005-x

42. Pal N, Bhaumik A. Soft templating strategies for the synthesis of mesoporous materials: Inorganic, organic-inorganic hybrid and purely organic solids. *Adv Colloid Interface Sci*. 2013;189-190:21-41. doi:10.1016/j.cis.2012.12.002

43. Malgras V, Tang J, Wang J, et al. Fabrication of nanoporous carbon materials with hard- and soft-templating approaches: a review. *J Nanosci Nanotechnol*. 2019;19(7):3673-3685. doi:10.1166/jnn.2019.16745

44. Zhang Z, Qin M, Jia B, et al. Facile synthesis of novel bowl-like hollow carbon spheres by the combination of hydrothermal carbonization and soft templating. *Chem Commun*. 2017;53:2922. doi:10.1039/c7cc00219j

45. De S, Balu AM, Van Der Waal JC, Luque R. Biomass-derived porous carbon materials: synthesis and catalytic applications. *ChemCatChem*. 2015;7(11):1608-1629. doi:10.1002/cctc.201500081

46. Yang Z, Zhang Y, Schnepp Z. Soft and hard templating of graphitic carbon nitride. *J Mater Chem A*. 2015;3(27):14081-14092. doi:10.1039/c5ta02156a

47. Gao Y, Yue Q, Gao B, Li A. Insight into activated carbon from different kinds of chemical activating agents: a review. *Sci Total Environ*. 2020;746:141094. doi:10.1016/j.scitotenv.2020.141094

48. Wu T, Wang G, Dong Q, et al. Starch derived porous carbon nanosheets for high-

performance photovoltaic capacitive deionization. *Environ Sci Technol*. 2017;51(16):9244-9251. doi:10.1021/acs.est.7b01629

49. Sevilla M, Fuertes AB. A green approach to high-performance supercapacitor electrodes: the chemical activation of hydrochar with potassium bicarbonate. *ChemSusChem*. 2016;9(14):1880-1888. doi:10.1002/cssc.201600426

50. Zhang Y, Song X, Xu Y, Shen H, Kong X, Xu H. Utilization of wheat bran for producing activated carbon with high specific surface area via NaOH activation using industrial furnace. *J Clean Prod*. 2019;210:366-375. doi:10.1016/j.jclepro.2018.11.041

51. Wang L, Sun F, Hao F, et al. A green trace K2CO3 induced catalytic activation strategy for developing coal-converted activated carbon as advanced candidate for CO2 adsorption and supercapacitors. *Chem Eng J*. 2020;383:123205. doi:10.1016/j.cej.2019.123205

52. Mao Y, Xie H, Chen X, et al. A combined leaching and electrochemical activation approach to converting coal to capacitive carbon in molten carbonates. *J Clean Prod*. 2020;248:119218. doi:10.1016/j.jclepro.2019.119218

53. Kong J, Gu R, Yuan J, et al. Adsorption behavior of Ni(II) onto activated carbons from hide waste and high-pressure steaming hide waste. *Ecotoxicol Environ Saf*. 2018;156:294-300. doi:10.1016/j.ecoenv.2018.03.017

54. Gao Y, Yue Q, Xu S, Gao B. Activated carbons with well-developed mesoporosity prepared by activation with different alkali salts. *Mater Lett*. 2015;146:34-36. doi:10.1016/j.matlet.2015.01.161

55. Zhao C, Xu L, Hu Z, Qiu S, Liu K. Facile synthesis of selenium/potassium tartrate derived porous carbon composite as an advanced Li-Se battery cathode. *RSC Adv*. 2016;6(53):47486-47490. doi:10.1039/c6ra07837k

56. Li Q, Wu X, Zhao Y, et al. Nitrogen-doped hierarchical porous carbon through one-step activation of bean curd for high-performance supercapacitor electrode. *ChemElectroChem*. 2018;5(12):1606-1614. doi:10.1002/celc.201800230

57. Xi Y, Yang D, Qiu X, Wang H, Huang J, Li Q. Renewable lignin-based carbon with a remarkable electrochemical performance from potassium compound activation. *Ind Crops Prod*. 2018;124:747-754. doi:10.1016/j.indcrop.2018.08.018

58. Brito MJP, Veloso CM, Santos LS, Bonomo RCF, Fontan R da CI. Adsorption of the textile dye Dianix® royal blue CC onto carbons obtained from yellow mombin fruit stones and activated with KOH and H3PO4: kinetics, adsorption equilibrium and thermodynamic studies. *Powder Technol*. 2018;339:334-343. doi:10.1016/j.powtec.2018.08.017

59. Sun Y, Yue Q, Gao B, Wang Y, Gao Y, Li Q. Preparation of highly developed mesoporous activated carbon by H4P2O7 activation and its adsorption behavior for oxytetracycline. *Powder Technol*. 2013;249:54-62. doi:10.1016/j.powtec.2013.07.029

60. Cao L, Yu IKM, Tsang DCW, et al. Phosphoric acid-activated wood biochar for catalytic conversion of starch-rich food waste into glucose and 5-hydroxymethylfurfural. *Bioresour Technol*. 2018;267:242-248. doi:10.1016/j.biortech.2018.07.048

61. Liu H, Zhang J, Bao N, Cheng C, Ren L, Zhang C. Textural properties and surface chemistry of lotus stalk-derived activated carbons prepared using different phosphorus oxyacids: adsorption of trimethoprim. *J Hazard Mater*. 2012;235-236:367-375. doi:10.1016/j.jhazmat.2012.08.015

62. Liu L, Deng QF, Liu YP, Ren TZ, Yuan ZY. HNO3-activated mesoporous carbon catalyst for direct dehydrogenation of propane to propylene. *Catal Commun*. 2011;16(1):81-85. doi:10.1016/j.catcom.2011.09.005

63. Zhou Y, Shi W, Engler N, Nelles M. High-value utilization of kitchen waste derived hydrochar in energy storage regulated by circulating process water. *Energy Convers Manag*. 2021;229:113737. doi:10.1016/j.enconman.2020.113737

64. Liu D, Wang Y, Jia B, et al. Microwave-Assisted Hydrothermal Preparation of Corn Straw Hydrochar as Supercapacitor Electrode Materials. *ACS Omega*. 2020;5(40):26084-26093. doi:10.1021/acsomega.0c03605

65. Hasham A, Jahin H, El-Korashy S, et al. Hydrochar for Industrial Wastewater Treatment: An Overview on its Advantages and Applications. *Artic J Environ Anal Toxicol*. 2021;11(February):2021. doi:10.37421/2161-0525.21.11.626

66. Haris M, Khan MW, Paz-Ferreiro J, Mahmood N, Eshtiaghi N. Synthesis of functional hydrochar from olive waste for simultaneous removal of azo and non-azo dyes from water. *Chem Eng J Adv*. 2022;9:100233. doi:10.1016/j.ceja.2021.100233

67. Bligaard T, Nørskov JK. Heterogeneous catalysis. In: *Chemical Bonding at Surfaces and Interfaces*. Elsevier; 2008:255-321. doi:10.1016/B978-044452837-7.50005-8

68. Atadashi IM, Aroua MK, Aziz AA. Biodiesel separation and purification: a review. *Renew Energy*. 2011;36(2):437-443. doi:10.1016/j.renene.2010.07.019

69. Zhao, D. Y.; Feng, J. L.; Huo, Q. S.; Melosh, N.; Fredrickson, G. H.; Chmelka, B. F.; Stucky GD. Homogeneous vs heterogeneous catalysts. *Sceince*. Published online 1998:548-552. Accessed June 4, 2022. https://www.ethz.ch/content/dam/ethz/special-interest/chab/icb/van-bokhoven-group-dam/coursework/Catalysis/2017/Homogeneous_Heterogeoenous_catalysis_Mesoporous

Materials.pdf

70. Takkellapati S, Li T, Gonzalez MA. An overview of biorefinery-derived platform chemicals from a cellulose and hemicellulose biorefinery. *Clean Technol Environ Policy*. 2018;20(7):1615-1630. doi:10.1007/s10098-018-1568-5

71. Zou X, Zhu C, Wang Q, Yang G. Catalytic dehydration of hexose sugars to 5-hydroxymethylfural. *Biofuels, Bioprod Biorefining*. 2019;13(1):153-173. doi:10.1002/bbb.1932

72. Kruger JS, Choudhary V, Nikolakis V, Vlachos DG. Elucidating the roles of zeolite H-BEA in aqueous-phase fructose dehydration and HMF rehydration. *ACS Catal*. 2013;3(6):1279-1291. doi:10.1021/cs4002157

73. Li X, Peng K, Liu X, Xia Q, Wang Y. Comprehensive understanding of the role of brønsted and lewis Acid Sites in glucose conversion into 5-Hydromethylfurfural. *ChemCatChem*. 2017;9(14):2739-2746. doi:10.1002/cctc.201601203

74. Zhao J, Zhou C, He C, Dai Y, Jia X, Yang Y. Efficient dehydration of fructose to 5-hydroxymethylfurfural over sulfonated carbon sphere solid acid catalysts. *Catal Today*. 2016;264:123-130. doi:10.1016/j.cattod.2015.07.005

75. Villa A, Schiavoni M, Fulvio PF, et al. Phosphorylated mesoporous carbon as effective catalyst for the selective fructose dehydration to HMF. *J Energy Chem*. 2013;22(2):305-311. doi:10.1016/S2095-4956(13)60037-6

76. Zhang F, Liao J, Lu J, Niu J. Extensive incorporation of carboxyl groups into g-C3N4 by integrated oxygen doping and HNO3 oxidation for enhanced catalytic ozonation of para-chlorobenzoic acid and atrazine. *Sep Purif Technol*. 2021;256:117806. doi:10.1016/j.seppur.2020.117806

77. Lynch J. Physico-chemical analysis of industrial catalysts: a practical guide to characterisation. Published online 2003:305.

78. Lu W, Chung DDL. Oxidation protection of carbon materials by acid phosphate impregnation. *Carbon N Y*. 2002;40(8):1249-1254. doi:10.1016/S0008-6223(01)00297-4

79. Ahmadpour A, Do DD. The preparation of active carbons from coal by chemical and physical activation. *Carbon N Y*. 1996;34(4):471-479. doi:10.1016/0008-6223(95)00204-9

80. Wang L, Guo Y, Zou B, et al. High surface area porous carbons prepared from hydrochars by phosphoric acid activation. *Bioresour Technol*. 2011;102(2):1947-1950. doi:10.1016/j.biortech.2010.08.100

Appendix A - Materials and methods

A.1 Inductive Coupled Plasma – Optical Emission Spectrometry, ICP – OES

To perform the ICP-OES analysis, three calibration curves had to be prepared, for the calibration of phosphorus, one for each wavelength. Of those three curves, one was chosen because it had the highest R^2 value. Figure A.1 presents the calibration curves.

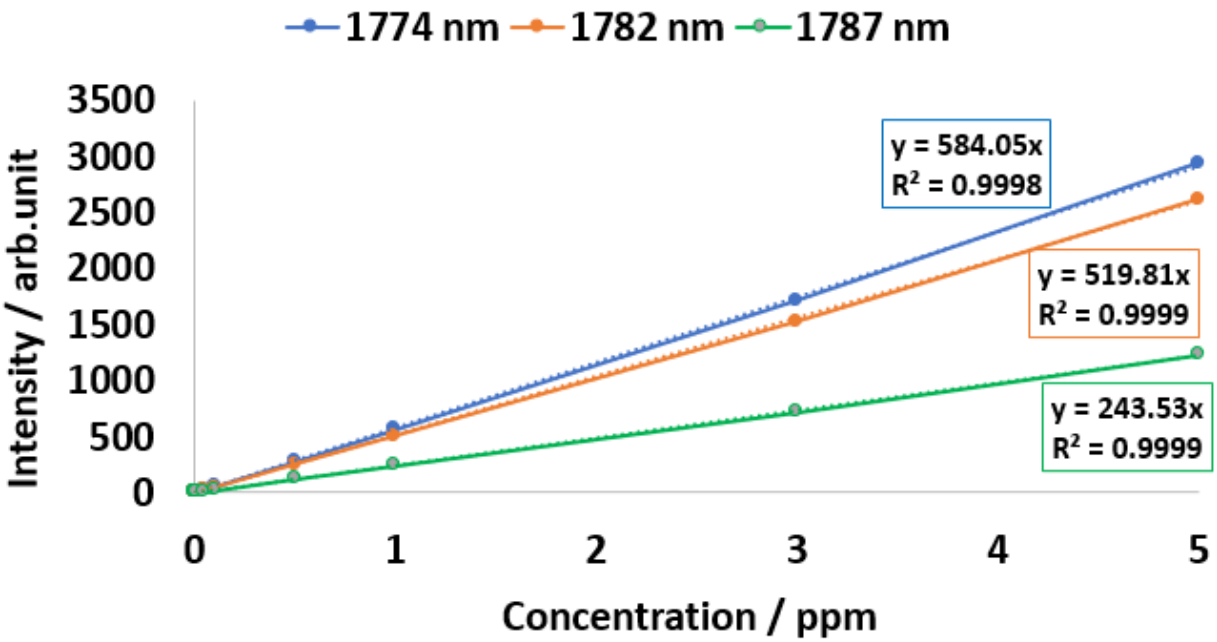

Figure A.1: ICP-OES calibration curves for phosphorus

According to Figure A.1, the curve that depicts the 1782 nm wavelength is the one that was chosen since it has the highest correlation factor (R^2). Thus, the remaining calculations for the concentration of phosphorus in the HTC_H_3PO_4 and HTC_H_3PO_4 materials were done using the slope and the interception of the orange curve.

A.2 High Performance Liquid Chromatography, HPLC

To calculate the number of moles of fructose and HMF of the samples took from the reaction of interest, two calibrations curves had to be determined, one for each substance. Each calibration curve was determined by using 5 stock solutions of fructose and HMF, with known concentrations. The solutions were analyzed in the HPLC equipment, and the areas of the peaks were correlated with the concentrations of fructose and HMF, which allowed for the development of the calibration curves using standard compounds obtained from Sigma-Aldrich.

Figure A.2: Calibration curves for a) Fructose and b) HMFa and b, detail the calibration curves of fructose and HMF, respectively.

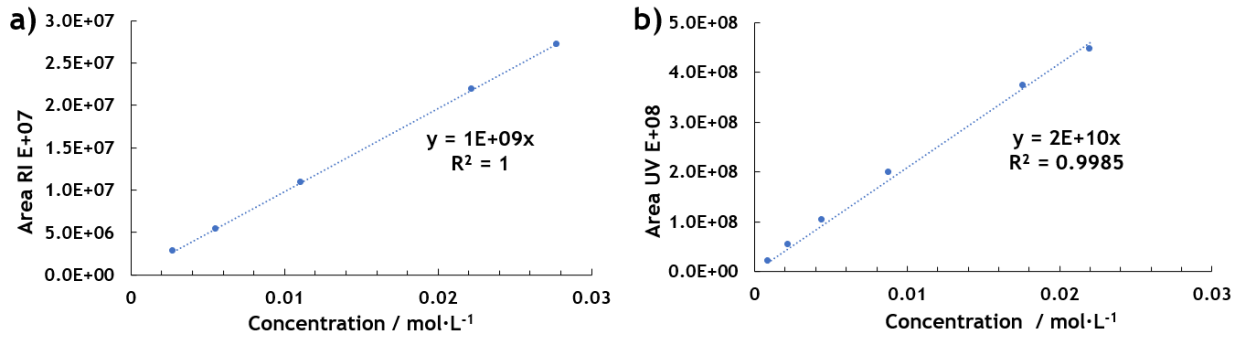

Figure A.2: Calibration curves for a) Fructose and b) HMF

Appendix B - Results and discussion

B.1 X-ray Photoelectron Spectroscopy, XPS

The XPS spectra for the nitrogen groups of and HTC and HTC_Carb_HNO_3, sulfur groups of material HTC_Carb_H_2SO_4 and phosphorus groups of material HTC_H_3PO_4_Carb, are detailed in Figure B.1a, b, c, d, e and f respectively.

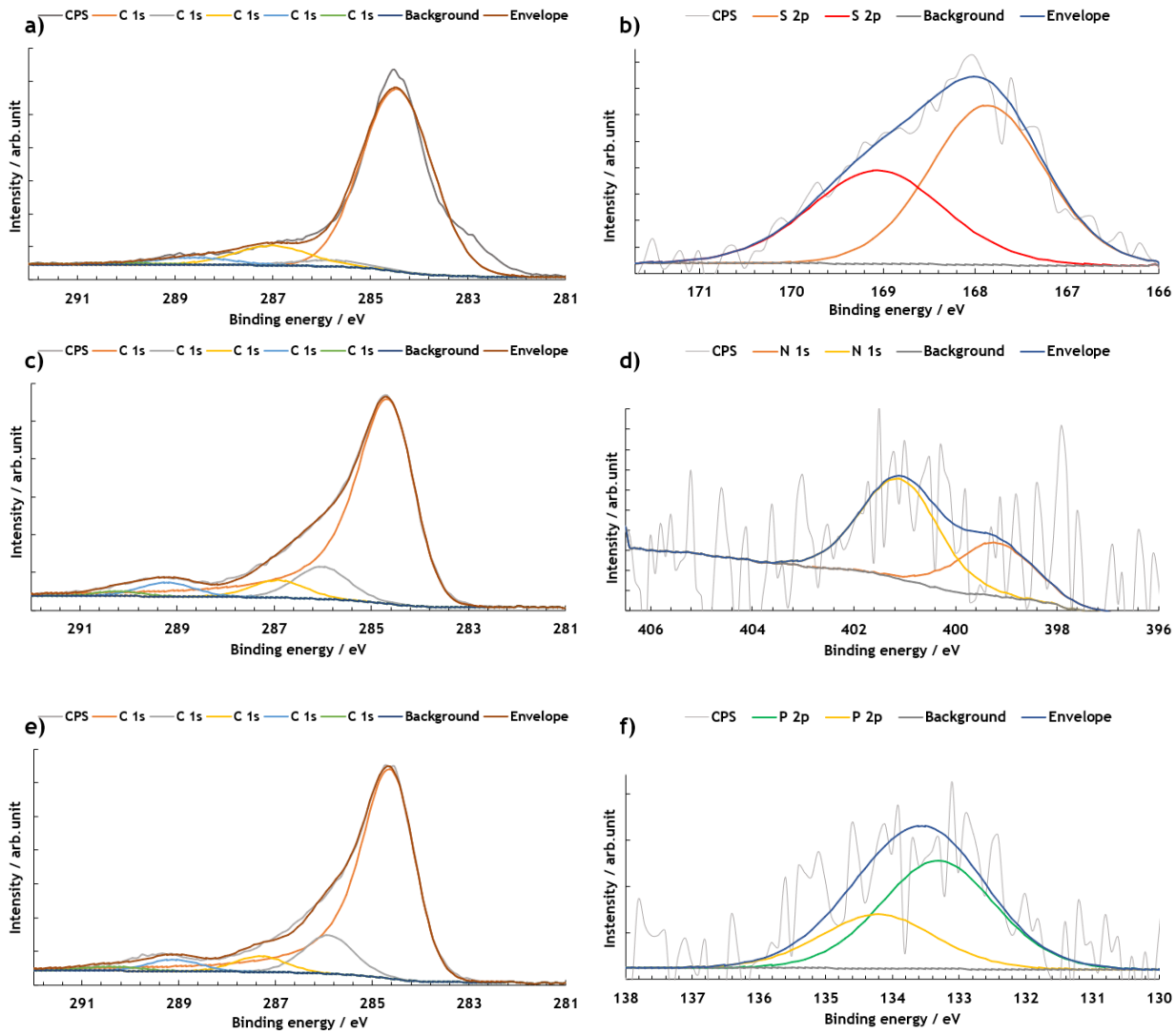

Figure B.1: XPS Spectra of a) C1s region of material HTC_Carb_H_2SO_4, b) S2p region of material HTC_Carb_H_2SO_4, c) C1s region of material HTC_Carb_HNO_3, d) N1s region of material HTC_Carb_HNO_3, e) C1s region of material HTC_H_3PO_4_Carb and f) P2p region of material HTC_H_3PO_4_Carb.

B.2 Thermogravimetric Analysis, TGA

The plots of the TG analysis containing the TG curve and the DTG (first derivative) for the materials HTC_Carb, HTC_Carb_O_2, HTC_CO_2, HTC_H_3PO_4, HTC_H_3PO_4_Carb, HTC_Carb_H_2SO_4, HTC_Carb_HNO_3 are presented in Figure B.2a, b, c, d, e, f and g, respectively.

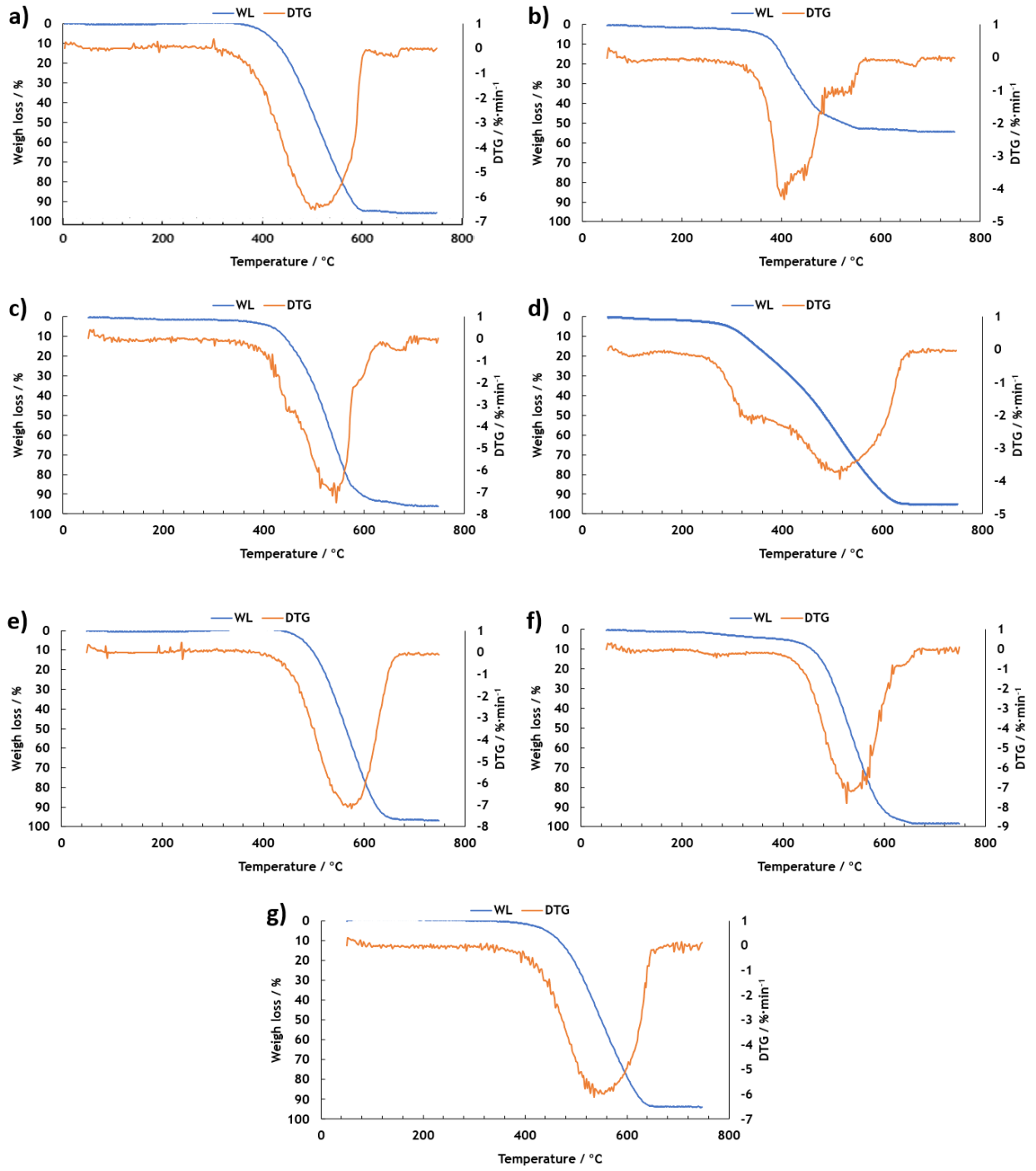

Figure B.2: TG and DTG of a) HTC_Carb, b) HTC_Carb_O_2, c) HTC_CO_2, d) HTC_H_3PO_4, e) HTC_H_3PO_4_Carb, f) HTC_Carb_H_2SO_4 and g) HTC_Carb_HNO_3